BEDROCK GEOLOGIC MAPS OF THE MOUNT HARPER-MIDDLE FORK AREA, VOLKMAR RIVER-HEALY RIVER AREA, GOODPASTER RIVER-SHAW CREEK AREA, AND THE RICHARDSON MINING DISTRICT, ALASKA

Evan Twelker, Rainer J. Newberry, Travis J. Naibert, Alicja Wypych, Michelle M. Gavel, Michael L. Barrera, David J. Szumigala, Conner M. Truskowski, Izzy P. Muller, Serena N. Fessenden, Noel J. Blackwell, David A. Harvey, and Alec D. Wildland

Preliminary Interpretive Report 2025-2

Granite in the Mount Harper Batholith at station 22Z246. Photo taken 7/24/2022 by D.J. Szumigala.

2025
STATE OF ALASKA
DEPARTMENT OF NATURAL RESOURCES
DIVISION OF GEOLOGICAL & GEOPHYSICAL SURVEYS

STATE OF ALASKA
Mike Dunleavy, Governor

DEPARTMENT OF NATURAL RESOURCES
John Boyle, Commissioner

DIVISION OF GEOLOGICAL & GEOPHYSICAL SURVEYS
Jennifer Athey, Acting State Geologist & Director

Publications produced by the Division of Geological & Geophysical Surveys are available to download from the DGGS website (dggs.alaska.gov). Publications on hard-copy or digital media can be examined or purchased in the Fairbanks office:

Alaska Division of Geological & Geophysical Surveys (DGGS)
3354 College Road | Fairbanks, Alaska 99709-3707
Phone: 907.451.5010 | Fax 907.451.5050
dggspubs@alaska.gov | dggs.alaska.gov

DGGS publications are also available at:

Alaska State Library, Historical
Collections & Talking Book Center
395 Whittier Street
Juneau, Alaska 99801

Alaska Resource Library and
Information Services (ARLIS)
3150 C Street, Suite 100
Anchorage, Alaska 99503

Suggested citation:
Twelker, Evan, Newberry, R.J., Naibert, T.J., Wypych, Alicja, Gavel, M.M., Barrera, M.L., Szumigala, D.J., Truskowski, C.M., Muller, I.P., Fessenden, S.N., Blackwell, N.J., Harvey, D.A., and Wildland, A.D., 2025, Bedrock geologic maps of the Mount Harper-Middle Fork area, Volkmar River-Healy River area, Goodpaster River-Shaw Creek area, and the Richardson mining district, Alaska: Alaska Division of Geological & Geophysical Surveys Preliminary Interpretive Report 2025-2, 39 p. https://doi.org/10.14509/31648

BEDROCK GEOLOGIC MAPS OF THE MOUNT HARPER-MIDDLE FORK AREA, VOLKMAR RIVER-HEALY RIVER AREA, GOODPASTER RIVER-SHAW CREEK AREA, AND THE RICHARDSON MINING DISTRICT, ALASKA

Evan Twelker[1], Rainer J. Newberry[1], Travis J. Naibert[1], Alicja Wypych[2], Michelle M. Gavel[2], Michael L. Barrera[1], David J. Szumigala[1], Conner M. Truskowski[1], Izzy P. Muller[3], Serena N. Fessenden[2], Noel J. Blackwell[2], David A. Harvey[2], and Alec D. Wildland[2]

ABSTRACT

The Mount Harper-Richardson project updates and improves upon the bedrock geologic mapping of a 7,988-sq-km (3,084-sq-mi) area north of the Richardson and Alaska highways between the communities of Salcha and Dot Lake in the Yukon-Tanana Uplands (YTU) of eastern Interior Alaska. The project's goals are: to better understand the geologic framework of known mineralization, to support the exploration and discovery of new mineral resources in the area, and to build scientific understanding of the geology of the YTU, one of Alaska's most active and important mineral belts. The project area has been a focus of gold exploration for several decades but also has additional significance for its potential to host critical minerals such as antimony, bismuth, tellurium, and tungsten.

Project work was completed by Alaska Division of Geological & Geophysical Surveys (DGGS) staff and collaborators during the 2022 and 2023 summer field seasons and draws on additional published and unpublished work completed during prior years by DGGS, University of Alaska, and U.S. Geological Survey staff. The project area is divided into four geologic map sheets, listed from east to west: the Mount Harper-Middle Fork area, the Volkmar River-Healy River area, the Goodpaster River-Shaw Creek area, and the Richardson mining district. The map units used across the four maps are described in this report.

INTRODUCTION

The Alaska Division of Geological & Geophysical Surveys (DGGS) Mineral Resources Section staff conducted bedrock geologic mapping of 7,988-sq-km (3,084-sq-mi) for the Mount Harper-Richardson project in the Yukon-Tanana Uplands (YTU) of eastern Interior Alaska during the 2022 and 2023 summer field seasons. Staff collected 3,178 rock stations, 407 geochemical samples, and 68 geochronology samples over 457 person-days of fieldwork. The Mount Harper-Richardson project includes four map areas with bedrock geology mapped at 1:100,000 scale and accompanying geologic map databases in the Alaska Geologic Mapping Schema.

[1] Alaska Division of Geological & Geophysical Surveys, 3354 College Road, Fairbanks, AK 99709
[2] *former* Alaska Division of Geological & Geophysical Surveys, 3354 College Road, Fairbanks, AK 99709
[3] Jackson School of Geosciences, University of Texas Austin, 23 San Jacinto Boulevard, Austin, TX 78712

The Mount Harper-Middle Fork area includes the high topography surrounding Mount Harper as well as the valleys of Joseph Creek, Molly Creek, and the Middle Fork of the Fortymile River, all within the southwest Eagle Quadrangle. The northern map boundary is the edge of the Yukon-Charley Rivers National Preserve. The map area borders published geologic maps of the Kechumstuk fault zone (Day and others, 2014) and the Big Delta B-1 Quadrangle (Day and others, 2007).

The Volkmar River-Healy River map area includes the Big Delta A-1 and A-2 quadrangles and parts of the Mt. Hayes D-1 and D-2 quadrangles. The area includes the Healy and Brink gold prospects. The map area borders the geologic maps of the Alaska Highway Corridor (Werdon and others, 2004), the Big Delta B-1 and B-2 quadrangles (Day and others, 2003, 2007), and the western Tanacross area (Wypych and others, 2024).

The Goodpaster River-Shaw Creek map area includes the area on both sides of the Goodpaster River north of its confluence with the Tanana River as well as the flats along Shaw Creek and includes parts of the Big Delta A-3, A-4, A-5, B-3, and B-4 quadrangles. The active Pogo gold mine is 15 km northeast of the map area. The map is divided from the Richardson mining district map area by the Shaw Creek fault. The map borders the Big Delta B-2 geologic map (Day and others, 2003) and the Salcha River-Pogo geologic map (Werdon and others, 2004) on the east and northeast sides, respectively.

The Richardson mining district map area includes the area northwest of Shaw Creek and the Shaw Creek fault. Initial fieldwork for this area was conducted in 2017 and 2018, and a preliminary geologic map (Twelker and others, 2021b) has been updated and incorporated into the current map area. The area includes the SAM (Naosi, Montecristo, Uncle Sam), Richardson, and Hilltop gold properties, and lies about 50 km west of the active Pogo gold mine.

DESCRIPTION OF MAP UNITS

IGNEOUS ROCKS

Slate Creek Intrusive Suite

Pɛfp FELSIC PORPHYRY (PALEOGENE)—Broadly scattered dikes and small stocks of granite, porphyritic granite, and granite porphyry. Phenocryst mineralogy includes quartz, alkali feldspar, plagioclase, and biotite; other primary minerals include garnet, and in some samples, white mica. Secondary minerals include sericite, chlorite, rutile, and local tourmaline. Groundmass grain size is 20–100 μm (0.02–0.1 mm) in porphyritic samples, and up to 0.4 mm in semi-equigranular samples. Magnetic susceptibility is low, 0.007–1.2 x 10^{-3} Système International (SI), with an average of 0–0.1 x 10^{-3} SI and a median of 0.07 x 10^{-3} SI. Timing of emplacement is constrained by U-Pb zircon crystallization ages of 56.8 ± 0.9 Ma (18WCW149; Twelker and O'Sullivan, 2021) and 62.53 ± 0.47 Ma (table 1;

22ADW256; Buchanan, Gavel, and others, 2025). We interpret this unit to represent the felsic component of a bimodal igneous suite associated with crustal extension.

Pzm MAFIC INTRUSIONS (PALEOGENE)—Rare, volumetrically minor dikes or small stocks of gabbro to diorite. Fine grained and equigranular to seriate. Primary mineralogy includes plagioclase, biotite, hornblende, augite, and lesser orthopyroxene, alkali feldspar, quartz, apatite, ilmenite, and magnetite. Secondary minerals include minor chlorite and sericite. Magnetic susceptibility at a single station is moderate, 0.23–0.47 x 10^{-3} SI, with a median value of 0.36 x 10^{-3} SI. Age of emplacement is constrained by a U-Pb zircon age of 56.6 ± 0.4 Ma (table 1; 22TJN285; Buchanan, Gavel, and others, 2025). Trace element geochemistry is consistent with a within-plate tectonic setting on diagrams of Pearce and Cann (1973) and Meschede (1986). We interpret this unit to be the intrusive equivalent of ca. 55 Ma basalts such as the Browns Hill Quarry basalt, unit Tb, of Newberry and others (1996).

Middle Fork Volcanic Complex

lKfv FELSIC VOLCANIC ROCKS (LATEST CRETACEOUS)—Rhyolite lithic-crystal tuff of the Middle Fork volcanic complex. Crystal fragments up to 3 mm in diameter include quartz, alkali feldspar, and plagioclase. Hornblende, biotite, and magnetite are also present as minor phenocryst or fragment phases. Lithic fragments comprise 0–5 percent of the rock and are subrounded to angular. Fiamme are present locally. Groundmass is sub-5 µm to 30 µm and may be fragmental or amorphous and isotropic. The magnetic susceptibility is generally high: 0.06–17 x 10^{-3} SI, with an average of 6.9 x 10^{-3} SI and a median of 8.1 x 10^{-3} SI; low values reflect hydrothermal alteration. This unit is expressed as a pronounced magnetic low on aeromagnetic surveys (Emond and MPX Geophysics, 2022), indicating that it retains reversely polarized magnetic remanence. Age of emplacement is constrained by a U-Pb zircon age of 70.0 ± 1.2 Ma 4 km east of the map area (sample 10ADb22; Bacon and others, 2014).

lKpg PORPHYRITIC GRANITE (LATEST CRETACEOUS)—An approximately 50-square-km granite intrusive body within the Middle Fork volcanic complex. Porphyritic, with phenocrysts 1- to 15-mm long, and groundmass is very fine grained to aphanitic, 20–200 µm (0.02–0.2 mm). Much of the body is fine grained enough to be described as granite porphyry. Phenocryst minerals include alkali feldspar, plagioclase, and biotite. Magnetite appears to be, at least in part, primary. Variably affected by secondary alteration, including sericite, chlorite, and calcite. The magnetic susceptibility is generally high: 0.1–15 x 10^{-3} SI, with an average of 5.7 x 10^{-3} SI and a median of 6.1 x 10^{-3} SI. Low values are due to hydrothermal alteration. Age of crystallization is constrained by a U-Pb zircon age of 69.7 ± 1.2 Ma determined for granite porphyry 2 km east of the map area (sample 10ADb17; Bacon and others, 2014).

Taurus Plutonic Suite

lKag

ALKALINE GABBRO (LATEST CRETACEOUS)—Fine-grained, holocrystalline, seriate augite-biotite-hornblende gabbro. Primary mineralogy includes hornblende, biotite, plagioclase, augite, alkali feldspar, and apatite. Titanite may be late magmatic or secondary. Augite is partially replaced by hornblende. Secondary mineralogy includes minor sericite replacement of plagioclase and chlorite replacement of biotite. Whole-rock geochemistry of this unit yields K_2O concentrations greater than 3 weight percent. Based on a small sample set (four), the magnetic susceptibility is relatively low: 0.04–0.7 x 10^{-3} SI, with an average of 0.37 x 10^{-3} SI and a median of 0.45 x 10^{-3} SI. Age of emplacement is constrained by an $^{40}Ar/^{39}Ar$ hornblende cooling age of 73.3 ± 0.8 Ma (table 1; 22RN184; Truskowski and others, 2025).

The alkaline gabbro mapped here is the northwesternmost member of a belt of widely scattered intrusions mapped in the upper Tanana Valley. It is equivalent to the latest Cretaceous parts of unit Kgb of Werdon and others (2019).

lKm

QUARTZ MONZODIORITE (LATEST CRETACEOUS)—Quartz monzodiorite to quartz monzonite, and lesser monzodiorite and diorite. Fine grained, hypidiomorphic, seriate, and locally porphyritic. Primary minerals include plagioclase, hornblende, biotite, alkali feldspar, quartz, apatite, and locally, augite. These compositions and mineralogy are based on hand sample observations with the support of handheld x-ray fluorescence data, but not whole-rock geochemistry or thin sections. Magnetic susceptibility is uniformly low: 0.033–0.6 x 10^{-3} SI, with an average of 0.24 x 10^{-3} SI and a median of 0.2 x 10^{-3} SI. Age of emplacement is inferred from spatial association with unit lKag alkaline gabbro, and from general compositional similarity to other latest Cretaceous, moderately alkaline igneous rocks in the region.

lKgd

GRANODIORITE (LATEST CRETACEOUS)—Two small (less than 5 sq km) stocks of granodiorite and lesser granite and quartz monzonite. Fine grained, seriate-to-equigranular, and locally, porphyritic. Primary mineralogy includes plagioclase, quartz, alkali feldspar, biotite, hornblende, magnetite, and titanite. Secondary minerals include minor replacement by chlorite and sericite. Based on a small sample set (six), the magnetic susceptibility is quite variable (0.06–7.0 x 10^{-3} SI, with an average of 1.8 x 10^{-3} SI and a median of 1.1 x 10^{-3} SI). Crystallization age is constrained by a U-Pb zircon age of 71.1 ± 1.4 Ma (21WCW008; Gavel and others, 2023) from just east of the Volkmar River-Healy River map area.

Fairbanks-Salcha Plutonic Suite

Kfsg

GRANITE OF FAIRBANKS-SALCHA SUITE (EARLY LATE CRETACEOUS)—Pluton- and stock-sized bodies of granite, as well as lesser granodiorite and tonalite, occurring in

the Salcha and Goodpaster River areas. Dominant textural variant is medium grained and porphyritic, with alkali feldspar phenocrysts 10- to 20-mm long; fine- and medium-grained equigranular variants are also included in this unit. Primary minerals include quartz, alkali feldspar, plagioclase, biotite, hornblende (minor, locally present), and ilmenite. Secondary minerals include chlorite, white mica, and calcite. Granite of the Fairbanks-Salcha suite is notable for its low magnetic susceptibility (0.001–0.9 x 10^{-3} SI, with an average of 0.11 x 10^{-3} SI and a median of 0.07 x 10^{-3} SI). Age of crystallization is constrained by a U-Pb zircon age of 92.4 ± 0.6 Ma (Birch Lake pluton; Twelker and O'Sullivan, 2021), among others.

Kfsgd GRANODIORITE OF FAIRBANKS-SALCHA SUITE (EARLY LATE CRETACEOUS)—Small plutons or stocks of seriate, fine-grained granodiorite, and lesser tonalite intruding the Shaw Creek and Goodpaster River areas. Primary mineralogy includes plagioclase, alkali feldspar, quartz, biotite (1–30 percent), and hornblende (1–20 percent); secondary minerals include variable chlorite and sericite. Magnetic susceptibility is low, but slightly higher than Fairbanks-Salcha suite granite (unit Kfsg): 0.02–1.2 x 10^{-3} SI, with an average of 0.16 x 10^{-3} SI and a median of 0.14 x 10^{-3} SI. A U-Pb zircon sample yielded a crystallization age of 90.8 ± 0.8 Ma (table 1; 22Z299; Buchanan, Gavel, and others, 2025).

Kfsp PORPHYRY OF FAIRBANKS-SALCHA SUITE (EARLY LATE CRETACEOUS)—Dike- to stock-sized bodies of fine-grained, porphyritic rocks of granite to granodiorite composition. Phenocrysts, generally less than 10 mm, include quartz, alkali feldspar, plagioclase, biotite, and local hornblende; groundmass grain size is 0.05 to 0.2 mm (50–200 µm). Secondary minerals include variably abundant chlorite, sericite, and pyrite. Magnetic susceptibility is generally low, but variable: 0.001–5.2 x 10^{-3} SI, with an average of 0.35 x 10^{-3} SI and a median of 0.1 x 10^{-3} SI. Crystallization age is based on a U-Pb zircon age of 92.0 ± 0.7 Ma (Democrat Dike; Twelker and O'Sullivan, 2021).

Kfsqd QUARTZ DIORITE OF FAIRBANKS-SALCHA SUITE (EARLY LATE CRETACEOUS)—Small stocks or plutons with compositions including quartz monzodiorite, quartz diorite, and diorite mapped in the lower Goodpaster River area, east of Shaw Creek. Typically fine grained, seriate-to-equigranular, and locally porphyritic. Primary minerals include plagioclase, alkali feldspar, quartz, biotite (10–15 percent), augite, and lesser orthopyroxene (0.5–20 percent), hornblende (5–10 percent; rimming pyroxenes), apatite, ilmenite, and local magnetite. Locally present secondary minerals include actinolite, chlorite, and calcite; titanite is likely secondary. Magnetic susceptibility is the highest of this suite: 0.03–5.2 x 10^{-3} SI, with an average of 0.57 x 10^{-3} SI and a median of 0.34 x 10^{-3} SI. A sample from this unit yielded a U-Pb zircon age of 98.57 ± 0.55 Ma (table 1; 22SNF222; Buchanan, Gavel, and others, 2025).

Kfsmg WHITE MICA-BEARING GRANITE OF FAIRBANKS-SALCHA SUITE (EARLY LATE CRETACEOUS)—Small stocks, plutons, and dikes of peraluminous granite occurring mostly between Salcha River and Shaw Creek. Equigranular, fine grained (0.5–3 mm), and

grades into local aplitic and pegmatitic zones in outcrop. Characterized by 5–10 percent primary (magmatic) white mica, as well as rare, fine-grained primary garnet in some samples; biotite is also locally present. Secondary minerals include locally intense sericite replacement of feldspar, tourmaline, and sulfide minerals. Magnetic susceptibility is uniformly low: 0.002–0.48 x 10^{-3} SI, with an average of 0.08 x 10^{-3} SI and a median of 0.04 x 10^{-3} SI.

The age of igneous crystallization of this unit is incompletely constrained. Naibert and others (2018) report an $^{40}Ar/^{39}Ar$ cooling age of 100.0 ± 0.7 Ma on magmatic muscovite from dike float at the Naosi gold deposit. A sample of a pervasively sericitized granitic dike that probably initially contained magmatic white mica yielded a U-Pb zircon age of 93.12 ± 0.87 Ma (table 1; 22MLB313; Buchanan, Gavel, and others, 2025), while $^{40}Ar/^{39}Ar$ dating of the sericite in the same sample returned a weighted mean age of 100.6 ± 1.0 (8 of 16 fractions) and an integrated age of 94.69 ± 0.06 Ma (22MLB313; Truskowski and others, 2025). One explanation for the discrepancy between the white mica and zircon ages is that excess argon may be present.

Gardiner Plutonic Suite

Kgt

TONALITE OF GARDINER SUITE (MID-CRETACEOUS)—Within the southern part of the Volkmar River-Healy River map area, this unit comprises a single stock of fine-grained, seriate tonalite. Primary mineralogy includes plagioclase, quartz, minor alkali feldspar, biotite (10–15 percent), hornblende (4 percent), and magnetite. Secondary minerals include chlorite, sericite, and epidote as low-intensity replacements. The median magnetic susceptibility of this unit is 7.2 x 10^{-3} SI. Age control is given by a U-Pb zircon age of 93.1 ± 0.8 Ma (table 1; 22IPM145; Buchanan, Gavel, and others, 2025). This unit is distinguished from Harper suite granodiorite (unit Khgd) by its younger crystallization age; it is distinguished from coeval rocks of the Fairbanks-Salcha plutonic suite by its elevated magnetic susceptibility. This unit corresponds to unit Ktn (tonalite) of Werdon and others (2019).

Harper Plutonic Suite

Khg

GRANITE OF HARPER SUITE (LATE EARLY CRETACEOUS)—Stock- to batholith-scale bodies of granite and lesser quartz monzonite and granodiorite and rare intermediate and mafic rocks. Typically fine to medium and locally coarse grained, equigranular to seriate, and locally porphyritic. Primary mineralogy includes quartz, alkali feldspar, plagioclase, and biotite (1–10 percent). Muscovite, magnetite, garnet, and hornblende occur as primary minerals in a minority of samples. Secondary minerals include chlorite, epidote, and sericite as partial replacements of primary phases. The Harper plutonic suite is characterized by a broad range of magnetic susceptibility that is independent of degree of fractionation; the granite unit ranges from 0.001 to 47 x 10^{-3} SI, with an average of 1.1 x

10^{-3} SI and a median of 0.14 x 10^{-3} SI. Age of crystallization is constrained by a U-Pb zircon age of 108.7 ± 2.2 Ma (18ADK080; Holm-Denoma and others, 2020).

Khgd GRANODIORITE OF HARPER SUITE (LATE EARLY CRETACEOUS)—Principally a batholith of roughly 500 sq km in exposed extent, plus smaller bodies in the vicinity. Granodiorite and minor tonalite are the most abundant lithologies, with up to 20 percent granite. Rare intermediate and mafic composition rocks also occur. Typically fine to medium grained and seriate, but in some cases porphyritic with a very fine grained groundmass. Primary minerals in granodiorite phase include plagioclase, quartz, alkali feldspar, biotite (10–15 percent), hornblende (1–5 percent), and in most samples, magnetite (0.3–2 percent). Augite, partially replaced by hornblende, is locally present. Secondary minerals include chlorite (variably replacing biotite and hornblende), biotite (locally replacing hornblende), sericite (variably replacing plagioclase cores), epidote, and local calcite. Magnetic susceptibility is much higher (0.02–31 x 10^{-3} SI, with an average of 7.2 x 10^{-3} SI and a median of 6.5 x 10^{-3} SI) than that of typical Harper granite (unit Khg). Age of crystallization is constrained by multiple U-Pb zircon ages ca. 106–110 Ma, including 107.7 ± 1.45 Ma (14ATe125; Todd and others, 2023).

Khgp GRANITE PORPHYRY OF HARPER SUITE (LATE EARLY CRETACEOUS)—Fine-grained, porphyritic intrusions of granite to tonalite composition cut the Mount Harper batholith as a northeast-trending linear swarm of dikes traceable for 13 km in the area northeast of Mount Harper. Characteristic phenocryst phases are quartz, alkali feldspar, plagioclase, and biotite. Groundmass is 10–50 μm, and spherulite devitrification textures are present in some samples. Secondary minerals include sericite after plagioclase, chlorite after biotite, and calcite. Magnetic susceptibility is variable: 0.015–13 x 10^{-3} SI, with an average of 2.1 x 10^{-3} SI and a median of 0.23 x 10^{-3} SI. The age of crystallization is constrained by a U-Pb zircon age of 107.5 ± 0.5 Ma (table 1; 22ET061; Buchanan, Gavel, and others, 2025).

Napoleon Creek Plutonic Suite

Jg NAPOLEON CREEK SUITE PLUTONIC SUITE UNDIVIDED (EARLY JURASSIC)—Unit includes one small intrusion on the eastern edge of the Mount Harper-Middle Fork map area, which is differentiated from mid-Cretaceous plutons based on its higher hornblende percentage. The intrusion is at the western end of a belt of plutons mapped as Mzh by Foster (1976), which has a U-Pb zircon age of 186.1 ± 0.87 Ma from a sample 11 km east of the map area (Todd and others, 2023). Regionally, this unit consists of multiple Early Jurassic intrusions in the Eagle Quadrangle (Foster, 1976; Werdon and others, 2001; Day and others, 2014) and northwest Tanacross Quadrangle (Naibert and others, 2024). These intrusions have U-Pb zircon ages of 181–191 Ma (Day and others, 2014) and were assigned by Naibert and others (2024) to the Napoleon Creek plutonic suite. Rock types include both alkalic

plutons, ranging from syenite to quartz monzodiorite, as well as calc-alkalic granodiorite and granite. Ages of approximately 183–185 Ma for granodiorite, granite, and quartz syenite suggest temporal overlap of quartz-rich and quartz-poor intrusions (Gavel and others, 2023). Magnetic susceptibility, reported by Naibert and others (2024) for similar rocks to the east, is usually moderate: 0.05–10 x 10^{-3} SI (average 4.5 x 10^{-3} SI) for quartz-rich rocks and slightly higher, 0.3–40 x 10^{-3} SI (average 7.7 x 10^{-3} SI), for quartz-poor rocks.

METAMORPHIC ROCKS

METAMORPHIC ROCKS OF THE YUKON-TANANA TERRANE

Klondike Assemblage

The Klondike assemblage consists of Middle to Late Permian metavolcanic rocks and related volcaniclastic metasediments (Colpron and others, 2006) with continental arc geochemistry (Piercey and others, 2006). The age of this assemblage is based on regional felsic schist samples yielding Permian zircon ages (Jones and O'Sullivan, 2020; Wildland and others, 2021). The assemblage underlies much of the Klondike region in the Yukon and extends into easternmost Alaska. Contacts between the Klondike assemblage and other allochthonous Yukon-Tanana terrane units are likely Triassic-Jurassic thrust faults. The Klondike units are also in low-angle fault contact with the parautochthonous Lake George assemblage in the Ladue River region southeast of the project area (Twelker and others, 2021a). Coeval intrusions, now orthogneiss, of the Sulphur Creek plutonic suite intrude the Klondike assemblage and other allochthonous units (Beranek and Mortensen, 2011) but were not mapped in the project area.

Pkmb — METABASITE OF KLONDIKE ASSEMBLAGE (PERMIAN)—Dark-gray to dark-green schistose unit consisting of fine-grained mafic to intermediate greenschist and thin interlayered quartzite. Mineralogy of the unit includes 10–30 percent chlorite, up to 40 percent actinolite, up to 40 percent albite, up to 20 percent epidote and (or) clinozoisite, up to 20 percent calcite, up to 10 percent quartz, up to 5 percent white mica, up to 0.5 percent magnetite, and rare disseminated sulfides. The unit has a moderate magnetic susceptibility: 0.01–1.6 x 10^{-3} SI, with an average of 0.28 x 10^{-3} SI and a median of 0.3 x 10^{-3} SI.

Pks — SCHIST OF KLONDIKE ASSEMBLAGE (PERMIAN)—A mixed unit consisting of felsic schist interpreted as metarhyolite, as well as chlorite schist and muscovite schist of mixed sedimentary and volcanic protoliths, and impure marble layers. Unit also contains minor quartzite, porphyroclastic orthogneiss, and rare metaconglomerate. Outcrops are generally pale green to dark green to gray and grain size is 0.1–2 mm. Layers are schistose and crenulated on the sub-centimeter scale, and the dominant foliation is often folded at the decimeter to meter scale. Greenschist facies mineralogy and the relatively fine grained, schistose texture suggest that this unit never reached the amphibolite-facies conditions reached by the Fortymile River assemblage. Mineralogy includes 30–90 percent quartz, up

to 40 percent actinolite, up to 50 percent albite, up to 35 percent muscovite, up to 20 percent biotite, up to 30 percent chlorite, and up to 15 percent epidote. Schist is locally iron (Fe) stained and contains traces of pyrite along fracture surfaces and veinlets. The unit has a generally low magnetic susceptibility: 0.003–1.1 x 10^{-3} SI, with an average of 0.15 x 10^{-3} SI and a median of 0.1 x 10^{-3} SI. Felsic schist from the Klondike assemblage in the Ladue River area yielded U-Pb zircon ages of 256.7 ± 5.8 and 261.4 ± 5.8 Ma (Wildland and others, 2021; Twelker and others, 2021a).

Nasina Assemblage

The Nasina assemblage is a greenschist- to amphibolite-facies metasedimentary package that is generally interpreted to be in thrust contact with the Fortymile River assemblage. The two assemblages are broadly interpreted to be different facies of the same overall lithotectonic assemblage—the Finlayson assemblage—in the Yukon (Colpron and others, 2006). Szumigala and others (2002) report local biotite, kyanite, and pyrophyllite, implying the rocks have been metamorphosed to upper greenschist facies in eastern Alaska. Felsic lithologies interlayered within this unit have yielded zircon U-Pb ages of approximately 349–359 Ma (Dusel-Bacon and others, 2006) and about 348 Ma (Yukon Geological Survey, 2019). Cooling ages determined by $^{40}Ar/^{39}Ar$ thermochronology are Middle Jurassic or older (Dusel-Bacon and others, 2002; Truskowski and others, 2025).

MDnm METABASITE OF THE NASINA ASSEMBLAGE (MISSISSIPPIAN to DEVONIAN)—This unit is mapped in a small area southeast of the Middle Fork Fortymile River; it includes fine-grained greenschist with mafic protoliths and variable degrees of fabric development. The unit is metamorphosed to greenschist facies in the project area. Typical mineralogy includes chlorite, actinolite, epidote, albite, titanite, clinozoisite, calcite, and up to 1 percent pyrite. Biotite was not observed in the mapped metabasite unit but was observed in metasedimentary rocks with interlayered greenschist and greenstone similar to this unit. Magnetic susceptibility is variably high: 0.07–39 x 10^{-3} SI, with an average of 1.8 x 10^{-3} SI and a median of 0.28 x 10^{-3} SI.

MDnms METASEDIMENTARY ROCKS OF THE NASINA ASSEMBLAGE (MISSISSIPPIAN to DEVONIAN)—The Nasina assemblage metasedimentary rocks include chlorite-albite-muscovite schist, chlorite-biotite-muscovite schist, albite-muscovite-quartz schist, graphitic-quartz schist, variably carbonaceous phyllite, banded to massive gray to dark-gray quartzite, and metamafic to intermediate schist. The different lithologies are locally interlayered on a centimeter scale. The unit is metamorphosed to greenschist facies in the project area. Foliation is well-developed and locally crenulated. Typical minerals present include quartz, muscovite, chlorite, biotite, albite, clinozoisite-epidote, actinolite, and potassium feldspar. Metamafic schist is locally calcite rich. Rare metaconglomerate with pebble-sized clasts and rare, thin marble layers are also present in the unit. Fine-grained

greenstone and greenschist layers with mafic to intermediate protoliths and moderate to absent fabric, as in unit MDnm, are interlayered but generally too thin to be shown at the map scale. Metafelsic layers were noted at a few stations and are interpreted to be metamorphosed dacitic to rhyolitic volcanic rocks; these are too thin to show as a separate map unit. The Nasina assemblage is distinguished by much more abundant carbonaceous layers than are present in metasedimentary units in either the Fortymile River assemblage or the Klondike assemblage. Magnetic susceptibility is generally low, but variable (due to the intermixed metamafic rocks): 0.004–3.8 x 10^{-3} SI, with an average of 0.12 x 10^{-3} SI and a median of 0.06 x 10^{-3} SI.

Fortymile River Assemblage

The Fortymile River assemblage comprises a heterogeneous group of epidote-amphibolite-facies metamorphic lithologies composed of metasedimentary rocks interlayered with amphibolite and lesser orthogneiss. Regionally, the age of this assemblage is constrained by datable interlayered lithologies. Zircon U-Pb ages of approximately 355 to 341 Ma were obtained from orthogneiss interpreted as having a volcanic protolith (Dusel-Bacon and others, 2006). Other orthogneiss layers, often with coarser textures, yielded Permian zircon U-Pb ages and are interpreted to have plutonic protoliths (Jones and others, 2017) intruded contemporaneously with Klondike assemblage arc magmatism. A thick marble layer located in the headwaters of Alder Creek in the Tanacross D-2 Quadrangle, 90 km east of the project area, yielded a mid-Mississippian to early Permian conodont age (Dusel-Bacon and Harris, 2003). This assemblage is a part of the Yukon-Tanana terrane as defined by Dusel-Bacon and others (2006) and is correlative with portions of the Finlayson assemblage of Colpron and others (2006) in the Yukon. The boundary between the allochthonous Fortymile River assemblage and the parautochthonous Lake George assemblage is interpreted as a regionally significant low-angle structure with northwest–southeast-directed extensional displacement (Dusel-Bacon and others, 2015, and references therein). This low-angle boundary is segmented by later high-angle faulting in many areas, including in the Mount Harper-Middle Fork map area. The Fortymile River assemblage is characterized by Jurassic $^{40}Ar/^{39}Ar$ cooling ages (Dusel-Bacon and others, 2002; Jones and others, 2017; Naibert and others, 2018; Jones and Benowitz, 2020).

MDfms METASEDIMENTARY ROCKS OF THE FORTYMILE RIVER ASSEMBLAGE (MISSISSIPPIAN to DEVONIAN)—A heterogeneous unit consisting of interlayered schist, quartz schist, quartzite, and paragneiss, with subordinate impure marble. Interlayered orthogneiss and amphibolite layers are not individually mappable in the unit. Minor marble or impure marble layers with white, yellow, gray, and bluish gray colors contain 35–95 percent calcite, 0–65 percent dolomite, and 5–50 percent quartz. Marble layers are centimeters to decimeters thick. Similar marble layers are more common in the Taylor Mountain map area to the east (Naibert and others, 2024). Meta-pebble-conglomerate layers are present locally. The unit also contains rare hornblende-bearing

muscovite schist with hornblende porphyroblasts along foliation planes. Schist and quartz schist contain 3–55 percent muscovite, 0–30 percent biotite, 20–70 percent quartz, 5–40 percent feldspar (dominantly plagioclase), and 0–10 percent garnet. Garnet porphyroblasts are typically 1–3 mm in diameter and are commonly altered to chlorite along fractures and grain edges. Schistosity is defined by muscovite, variably chloritized biotite, and fine-grained quartz ribbons. Plagioclase is partly altered to sericite. Paragneiss samples have similar mineralogy, with higher feldspar abundance (up to 50 percent) and less muscovite (5–25 percent). Gneissic banding is defined by quartz- and feldspar-rich layers separating quartz- and mica-rich layers. Quartzite contains 85–95 percent quartz, with 0.05–1 mm anhedral grains. Quartzite foliation is defined by elongate quartz grains and 1–10 percent micas, commonly muscovite and lesser biotite with minor chlorite replacement of biotite. Magnetic susceptibility is mostly low: 0.004–3.6 x 10^{-3} SI, with an average of 0.22 x 10^{-3} SI and a median of 0.15 x 10^{-3} SI. Available U-Pb zircon ages from interlayered orthogneiss interpreted as metavolcanic rocks are ca. 355–341 Ma (Dusel-Bacon and others, 2006; Wypych and others, 2020), suggesting that sedimentation was Mississippian or older.

MDfp

PARAGNEISS OF THE FORTYMILE RIVER ASSEMBLAGE (MISSISSIPPIAN to DEVONIAN)—Paragneiss with subordinate interlayered schist, quartz schist, amphibolite, orthogneiss, and thin marble. Grain sizes are 0.01–10 mm with moderate to strong foliation. Typical paragneiss and schist mineralogy includes up to 70 percent quartz, up to 20 percent biotite, up to 10 percent chlorite, up to 40 percent feldspar, up to 55 percent muscovite, up to 5 percent calcite, up to 5 percent garnet, up to 5 percent hornblende, and trace magnetite. Magnetic susceptibility is generally low: 0.1–1.5 x 10^{-3} SI, with an average of 0.17 x 10^{-3} SI and a median of 0.13 x 10^{-3} SI. Similar units have been described in the Eagle A-1 and A-2 quadrangles (Szumigala and others, 2002; Werdon and others, 2001) as schist and paragneiss (pMsg) and gneiss (pMg).

MDfa

AMPHIBOLITE OF THE FORTYMILE RIVER ASSEMBLAGE (MISSISSIPPIAN to DEVONIAN)—Amphibolite interlayered with subordinate amphibole-bearing gneiss and orthogneiss. The amphibolite is green to dark green to dark gray, weathering pale green to brown, with foliated or gneissic texture. Foliation is defined by aligned amphibole, biotite, and (or) chlorite. Hornblende and garnet locally form porphyroblasts. Grain sizes are 0.05 to 15 mm. Layers contain up to 65 percent amphibole (dominantly hornblende with less common retrograde actinolite), up to 45 percent plagioclase, up to 5 percent biotite, up to 5 percent garnet, up to 5 percent chlorite, up to 15 percent clinozoisite-epidote, up to 5 percent quartz, minor sericite alteration of plagioclase, minor magnetite and sulfides, and 2–3 percent calcite. Plagioclase compositions measured on the microprobe are less than 40 percent anorthite, which is distinctly lower than those measured in Lake George assemblage amphibolite samples (Newberry and Twelker, 2021). Hornblende is dominantly euhedral with grains ranging up to 15 mm long and is less commonly acicular. Disseminated pyrite is present in some outcrops. Plagioclase is generally interstitial.

Magnetic susceptibility is variably high: 0.4–18 x 10^{-3} SI, with an average of 1.2 x 10^{-3} SI and a median of 0.47 x 10^{-3} SI. Regionally, Fortymile River assemblage amphibolite samples yield predominantly volcanic arc trace element signatures with some within-plate signatures (Dusel-Bacon and others, 2009; Wypych and others, 2018). A sample from the Tanacross Quadrangle yielded a zircon U-Pb age of 336.9 ± 3.8 Ma, which is interpreted to be the age of the igneous protolith (Wypych and others, 2020).

MDfo ORTHOGNEISS OF THE FORTYMILE RIVER ASSEMBLAGE (MISSISSIPPIAN to DEVONIAN)—Dominantly fine- to medium-grained orthogneiss of intermediate to felsic composition with subordinate interlayered metasedimentary rocks and amphibolite. The orthogneiss is typically pale gray to light brown and moderately foliated, with a grain size of 0.01–3 mm. Gneissic textures are common; schistose textures are also present. Petrography shows weak to moderate foliation is normally defined by biotite and lesser muscovite. Mineralogy consists of 30–55 percent plagioclase, 10–35 percent alkali feldspar, 5–50 percent quartz, 0–40 percent hornblende, 2–20 percent biotite, 5–15 percent muscovite, and up to 15 percent chlorite (as replacement of biotite and hornblende). Accessory minerals include garnet, hematite, and magnetite. Magnetic susceptibility is generally low: 0.002–3.6 x 10^{-3} SI, with an average of 0.3 x 10^{-3} SI and a median of 0.23 x 10^{-3} SI. An orthogneiss in the northeast Tanacross Quadrangle yielded a zircon U-Pb igneous crystallization age of 341.1 ± 2.3 Ma and is correlative with this unit (Wypych and others, 2020).

PARAUTOCHTHONOUS METAMORPHIC ROCKS OF NORTH AMERICA

Butte Assemblage

Dusel-Bacon and others (2006) proposed this name for greenschist facies metasedimentary and lesser metavolcanic rocks that occur north of, and structurally overlying (?), amphibolite-facies rocks of the Lake George assemblage. Only metasedimentary rocks are seen in the project area.

MDbms METASEDIMENTARY ROCKS OF THE BUTTE ASSEMBLAGE (MISSISSIPPIAN to DEVONIAN)—A mixed greenschist facies metasedimentary unit consisting of approximately 40 percent phyllite to fine-grained schist, 20 percent quartz phyllite, 20 percent micaceous quartzite, and 20 percent metagrit. The latter displays a bimodal clastic texture, consisting of coarse quartz sand-sized grains in a silt-size matrix. Phyllitic schist is fine grained (maximum 0.5 mm), with 30–40 percent quartz (0.05–0.5 mm), 20–50 percent white mica (0.05–0.4 mm), 5–30 percent chlorite (0.03–0.3 mm), 5–15 percent albite (0.05–0.2 mm), 0–3 percent biotite (0.03–0.1 mm), and trace–1 percent ilmenite (0.03–0.1 mm). Quartz phyllite contains more quartz (60–75 percent) and less mica and chlorite. Quartzite contains yet more quartz (85–90 percent). Metagrit contains 10–30 percent rounded quartz grains (0.2–1.5 mm) in a 0.03–0.05 mm matrix dominated by chlorite and quartz with lesser albite, white mica, and biotite. Magnetic susceptibility is low: 0.023–0.79 x 10^{-3} SI,

with an average of 0.15 x 10^{-3} SI and a median of 0.12 x 10^{-3} SI. This unit is correlated with the Totatlanika schist in the upper Chena area (Smith and others, 1994) and with greenschist facies metagrit-bearing rocks (MDg and MDs) of the Salcha River-Pogo area (Werdon and others, 2004). A Devonian to Mississippian depositional age is inferred by association of Butte lithologies with metafelsic rocks yielding U-Pb crystallization ages of 364 ± 3 and 371 ± 7 Ma (Dussel-Bacon and others, 2004).

Fairbanks-Chena Assemblage

Dusel-Bacon and others (2006) named the (mostly) amphibolite-facies rocks that occur north of the greenschist-faces belt (Butte and Blackshell units) "Fairbanks-Chena assemblage." They noted that this assemblage contains more quartzite and calcareous rocks and less orthogneiss than the Lake George assemblage. The metamorphic grade of the Fairbanks-Chena assemblage appears to be epidote-amphibolite (Newberry and others, 1996); Lake George is of higher, upper amphibolite facies as evidenced by the common occurrence of garnet and local diopside in metamafic rocks (Newberry and Twelker, 2021). We have identified an area of Fairbanks-Chena assemblage in the Richardson mining district where Lake George assemblage was previously mapped (Dusel-Bacon and others, 2006), based on the presence of rocks of somewhat lower metamorphic grade and with a greater abundance of quartzite and calcareous rocks and lower abundance of orthogneiss than is typical of Lake George assemblage. The two assemblages appear to be in fault contact, with Lake George assemblage structurally beneath.

TrPzfcu META-ULTRAMAFIC ROCKS OF FAIRBANKS-CHENA ASSEMBLAGE (TRIASSIC? TO PALEOZOIC)—Twelve small (0.08–1.3 sq km), sinuous bodies in the northeast and one tiny (0.04 sq km) body in the south-central part of the Fairbanks-Chena assemblage mapped in the Richardson mining district. These are metamorphosed ultramafic rocks occurring as lenses mostly within the Fairbanks-Chena schist and gneiss unit. As drawn, the bodies contain about one-third non-ultramafic rocks; more detailed mapping would perhaps result in smaller bodies of entirely ultramafic rocks. The tiny south-central body is about 80 percent serpentine, 10 percent chromium (Cr)-rich chlorite, 4 percent magnetite, and 6 percent combined relict talc plus tremolite. The degree of serpentinization has obliterated its metamorphic history. The northeastern bodies, on the other hand, are much less serpentinized (1–30 percent) and are dominated by, or at least contain, relicts of an enstatite + anthophyllite assemblage, indicating crystallization under relatively low-pressure, high-temperature, middle amphibolite-facies conditions, consistent with sillimanite stability. The least-altered sample mostly consists of an assemblage of 30 percent anthophyllite (0.3–3 mm), 50 percent enstatite, and 10 percent Cr-chlorite; veins of olivine (Fo_{80-83}) + talc + tremolite constitute nearly 10 percent of the rock, and about 1 percent is late serpentine. More commonly, such rocks contain 45–80 percent olivine + talc + tremolite with 10–20 percent anthophyllite + enstatite + Cr-chlorite and 25–30 percent late serpentine. These minerals were confirmed by microprobe as part of this study. Magnetite

contents are relatively high (3–4 percent) but depend on the amount of low-Fe (talc and serpentine) minerals' destruction of higher-Fe (olivine and enstatite) minerals. Consequently, the magnetic susceptibility of this unit is generally higher than any other unit in the Richardson map area. However, because the unit in part contains non-ultramafic rocks, and poorly magnetic ultramafic rocks, the magnetic susceptibility (0.02–152 x 10^{-3} SI, with an average of 22 x 10^{-3} SI and a median of 20 x 10^{-3} SI) is quite variable. In part, the contacts of this unit are based on magnetic highs seen on aeromagnetic maps (Burns and others, 2020).

The ultramafic rocks were structurally(?) introduced into the Fairbanks-Chena sequence prior to amphibolite-facies metamorphism and so must be older than the (Cretaceous?) metamorphism. The only known source of ultramafic rocks in Interior Alaska is the Mississippian to Upper Triassic Seventymile terrane, approximately 75 km to the northeast, but how such rocks were slivered into the Fairbanks-Chena sequence is unknown. Thus, correlation of the meta-ultramafic rocks with the little-metamorphosed ultramafic rocks of the Seventymile terrane is uncertain.

MDfca

AMPHIBOLITE OF FAIRBANKS-CHENA ASSEMBLAGE (MISSISSIPPIAN to DEVONIAN)—Amphibolite to amphibole-rich orthogneiss is commonly present with other Fairbanks-Chena lithologies. It occurs as narrow discontinuous lenses throughout the Fairbanks-Chena schist and gneiss unit, and as individual occurrences too small to map. Based on field mapping, the unit is approximately 60 percent amphibolite, 20 percent granitic orthogneiss, 10 percent biotite-rich schist, and 10 percent granite (presumably dikes). The unit is dark green to gray, commonly weathers to brown, and is fine to coarse grained with a gneissic to schistose texture. The predominant rock type is biotite-hornblende amphibolite (some partially retrograded to greenschist facies) with a 0.1–6 mm grain size. Thin section examination shows that epidote-clinozoisite (not visible in hand specimen) is nearly ubiquitous, with 2–10 percent typical. Other minerals present include 35–65 percent hornblende (subhedral, 0.2–6 mm), 10–40 percent subhedral plagioclase (0.1–2.5 mm) partly to strongly altered to sericite (0.5–15 percent), 0–15 percent biotite (0.1–1 mm), 0.5–3 percent subhedral to euhedral titanite (0.03–0.4 mm), 0.3–2 percent euhedral apatite (0.03–0.2 mm), and 0.2–5 percent opaques (ilmenite + magnetite). Based on optical determinations, the plagioclase is approximately An_{25-35}. A sericite-rich sample also contains 1 percent chlorite, which is typically absent or present in trace amounts. The majority of known occurrences appear to represent epidote-amphibolite-facies conditions; however, an occurrence in the northeast corner of the Richardson mining district map appears to have been recrystallized at amphibolite facies. This sample contains variably aligned amphibole, zoned from magnesio-hornblende cores to ferro-tschermakite rims, high-Ca (An_{80-97}) plagioclase, and almandine garnet.

Magnetic susceptibility of the unit is moderate to high and variable (0.014–80 x 10^{-3} SI, with an average of 4.4 x 10^{-3} SI and a median of 0.46 x 10^{-3} SI), reflecting both the variety of rock types present and variable magnetite contents in amphibolite. In a few cases amphibolite bodies could be traced using aeromagnetic highs. This unit is correlated with Pzrp (amphibolite in the Chena River sequence) of Smith and others (1994) and Zfa (amphibolite in the Fairbanks schist unit) of Newberry and others (1996).

MDfco ORTHOGNEISS OF FAIRBANKS-CHENA ASSEMBLAGE (MISSISSIPPIAN to DEVONIAN)—Three large (8–10 sq km) coherent bodies and numerous smaller (0.03–1 sq km) bodies are present throughout the area of Fairbanks-Chena assemblage rocks mapped in the Richardson mining district. Based on samples collected during mapping, this unit consists of approximately 85 percent meta-igneous and 15 percent metasedimentary rocks, chiefly paragneiss and schist (described below). In many cases the two seem interstratified. Of the meta-igneous rocks, approximately five percent have gabbroic, diorite, or quartz diorite compositions, 10 percent have granodiorite or tonalite compositions, and 85 percent have granite compositions. Of the latter, approximately one-quarter contain 5–35 mm alkali feldspar porphyroclasts ("augen").

Granite orthogneiss is mostly fine to medium grained, locally mylonitic or schistose, with a typical grain size of 0.1–4 mm; rare alkali feldspar augen are up to 35 mm. The rocks are tan, light brown, and gray, and minimally to strongly weathered with varying degrees of chloritic and sericitic alteration. Their mineralogy includes 20–40 percent anhedral to subhedral alkali feldspar, commonly twinned and inclusion-rich; 20–35 percent subhedral plagioclase with polysynthetic twinning and minor to major sericite alteration; 25–40 percent subhedral to anhedral dynamically recrystallized quartz; 1–13 percent biotite (variably altered to chlorite); 0–10 percent muscovite; and (locally) up to 6 percent hornblende. Biotite and muscovite commonly define the foliation. Accessory minerals variably present include garnet, pyrite, magnetite, apatite, zircon, epidote, ilmenite, allanite, and titanite.

Granodiorite orthogneiss is similar but contains less alkali feldspar (10–15 percent) with maximum 3 mm grain size, and more plagioclase (40–45 percent) and biotite (14–16 percent). Secondary sericite and chlorite are present, but muscovite is absent. Tonalite, diorite, and quartz diorite orthogneiss basically lack alkali feldspar (0–3 percent) and contain significant hornblende (5–35 percent), 40–60 percent plagioclase, and 2–6 percent epidote, in addition to 12–18 percent biotite. Titanite (1–3 percent) and apatite (0.5–1 percent) are ubiquitous. Rocks of the unit have generally low, but variable, magnetitic susceptibility (0.002–13 x 10^{-3} SI, with an average of 0.49 x 10^{-3} SI and a median of 0.11 x 10^{-3} SI) as expressed by the considerably larger mean than median value. This is both due to variations in the granite orthogneiss and differences between typical granite orthogneiss and intermediate composition orthogneiss. Fairbanks-Chena orthogneiss is correlated

with unit Pzra (augen orthogneiss) in the upper Chena area (Smith and others, 1994) and unit Mog (orthogneiss) in the Fairbanks area (Newberry and others, 1996). A sample from the latter yielded a U-Pb crystallization age of 351 ± 2 Ma (Newberry and others, 1998). An augen orthogneiss from the Fairbanks-Chena assemblage in the southeast Circle Quadrangle (Dusel-Bacon and others, 2006) yielded a similar U-Pb crystallization age of 355 ± 4 Ma (Dusel-Bacon and others, 2003).

pMfccs CALC-SILICATE GNEISS OF FAIRBANKS-CHENA ASSEMBLAGE (PRE-MISSISSIPPIAN)—Metamorphic calc-silicate rocks are seen sporadically in the Fairbanks-Chena schist and gneiss unit (pMfcsg). Mappable bodies of calc-silicate gneiss mostly occur as a cluster in the north-central part of that unit and as two isolated lenses in the southwest part of the Richardson map. Based on field observations, the unit is about 60 percent calc-silicate rocks, 30 percent pale green rocks of uncertain mineralogy, and 10 percent granite. The known calc-silicate rocks are banded pale (diopside) to dark (amphibole) green and white (plagioclase + quartz), commonly with some brown (garnet ± vesuvianite) patches. Mineralogically, the calc-silicate rocks come in two varieties: quartz-poor (about two-thirds of occurrences) and quartz-rich (about one-third of occurrences). Both types contain diopside or hornblende, but rarely both. The quartz-poor rocks are somewhat finer grained (0.1–1 mm); quartz-rich rocks are coarser (0.1–3 mm) with more easily identified minerals. Quartz-poor types contain 3–25 percent quartz, 20–40 percent Ca-rich plagioclase (An_{50-70}), 30–40 percent diopside (or, less commonly, hornblende), 0–15 percent calcic garnet, 0–20 percent alkali feldspar, 0.5–2 percent titanite, 0–2 percent sericite (alteration of plagioclase), and 0–3 percent epidote-clinozoisite (alteration of garnet). Quartz-rich types contain 60–65 percent quartz, 15–20 percent Ca-rich plagioclase (An_{50-80}), 10 percent diopside or hornblende, 0–10 percent garnet, 0.5–1 percent titanite, 0–3 percent alkali feldspar, and 0–1.5 percent clinozoisite. The magnetic susceptibility of rocks in this unit is consistently low (0.022–0.65 x 10^{-3} SI, with an average of 0.24 x 10^{-3} SI and a median of 0.24 x 10^{-3} SI), in agreement with low opaque mineral abundances seen in thin section.

The southernmost calc-silicate gneiss lens is located within a kilometer of the 70-sq-km Birch Lake granite pluton; those calc-silicate rocks are likely of contact metamorphic origins. Some of the bodies in the northern cluster are similarly within 1–2 km of known granite bodies and likely of similar origins. However, the southwestern body is more than 5 km from known granite, and some of the northern cluster bodies are similarly distant. These are more likely to be regional metamorphic rocks, perhaps formed during the late, lower-pressure recrystallization seen in the nearby sillimanite-bearing schist and gneiss. This unit is correlated with unit Pzrcs (calc-silicate rocks of the Chena River sequence) of Smith and others (1994).

pMfcg GRAPHITIC ROCKS OF FAIRBANKS-CHENA ASSEMBLAGE (PRE-MISSISSIPPIAN)—A poorly exposed unit present in two discontinuous bands in the

northern body of Fairbanks-Chena assemblage rocks. As mapped, the unit is about half graphitic quartz-muscovite schist plus graphitic muscovite-quartz schist, with up to 10 percent graphite. The other half is non-graphitic rocks, commonly mica-quartz schist, with lesser altered granite, muscovite-plagioclase-quartz paragneiss, and calc-silicate paragneiss. However, given the generally poor outcrop preservation (mostly tiny chips) of the graphite-rich rocks, the unit may be dominantly graphitic. Magnetic susceptibility is low: 0.002–0.5 x 10^{-3} SI, with an average of 0.14 x 10^{-3} SI and a median of 0.12 x 10^{-3} SI. The unit is mapped in part by discontinuous conductivity zones seen in 900-Hz airborne electromagnetic maps (Burns and others, 2020). This unit is correlated with Pzrg (graphitic schist of the Chena River sequence) of Smith and others (1994).

pMfcm MARBLE OF FAIRBANKS-CHENA ASSEMBLAGE (PRE-MISSISSIPPIAN)—Impure marble is sporadically present in Fairbanks-Chena schist and gneiss; in a few cases it forms mappable bodies. Impure marble is light gray to light blueish green and fine to medium grained (0.1–0.8 mm), some with gneissic banding. The rock is typically 30–60 percent calcite; the remainder is a mix of quartz, clinozoisite, plagioclase, diopside, tremolite, and (or) chlorite. The magnetic susceptibility is low (0.11–0.5 x 10^{-3} SI, with an average of 0.17 x 10^{-3} SI and a median of 0.15 x 10^{-3} SI), but higher than typical quartzite, reflecting the presence of non-carbonate minerals. This unit is correlated with Pzrm (marble in Chena River sequence) of Smith and others (1994) and Zfm (marble in Fairbanks schist) of Newberry and others (1996).

pMfcq QUARTZITE OF FAIRBANKS-CHENA ASSEMBLAGE (PRE-MISSISSIPPIAN)—Quartzite is reported sporadically throughout the central and northern parts of the Fairbanks-Chena schist and gneiss unit. Where sufficiently common, it has been mapped as irregular lenses of unit pMfcq. This unit is problematic because fine-grained quartz is difficult to distinguish from fine-grained feldspar in the field. Of 12 samples field-identified as quartzite and subjected to further analysis, only four proved to be quartzite. The others contained relatively low SiO_2 (86–24 weight percent), and include siliceous calc-silicate gneiss, quartz-rich paragneiss, siliceous hornfels, silicified serpentinite, altered granite, and siliceous dolomitic marble. Based on these results and field identifications, the mapped unit is approximately half quartzite and quartz-rich paragneiss, one-quarter other fine-grained, mostly siliceous rocks, and one-quarter granitic rocks. Quartzite is gray to pale green and weathers light tan to orange; very fine grained to fine grained (0.01–0.5 mm); weakly foliated; and contains 80–87 percent quartz (anhedral, sometimes parted by thin mica layers), 1–10 percent white mica (some replacing feldspar), 1–5 percent biotite (slightly altered to chlorite), 5–15 percent feldspar (anhedral, locally stretched), and trace amounts of calcite, chlorite, pyrite, and iron oxide. Quartz-rich paragneiss is mostly coarser grained (0.1–2.5 mm) and contains 65–75 percent quartz, 3–10 percent muscovite, 2–7 percent biotite, 5–25 percent plagioclase (An_{20-30}) slightly altered to sericite, 0–6 percent alkali feldspar, and 0–3 percent garnet. Magnetic susceptibility of this unit is generally low, but highly variable (0.001–23 x

10^{-3} SI, with an average of 0.55 x 10^{-3} SI and a median of 0.1 x 10^{-3} SI), reflecting the wide variety of rock types in the unit. This unit is correlated with quartzite in the Chena River sequence (Smith and others, 1994) and in the Fairbanks schist (Newberry and others, 1996).

A distinctive quartzite unit is present at the LMS gold prospect, where drilling shows it dips moderately to the west (Hunter and Giroux, 2014). We tentatively assign this isolated quartzite to the Fairbanks-Chena assemblage on the basis of its graphite content and its association with garnet schist and calc-silicate gneiss, as described by Hunter and Giroux (2014). The LMS quartzite exposure is approximately 90 percent graphitic quartzite and 10 percent graphitic muscovite-quartz schist. Quartzite here is dark gray to black, fine grained (0.1–1 mm), weakly foliated, and variably brecciated. It consists of 90–95 percent quartz, 3–8 percent muscovite, and 1–3 percent graphite, with 0.5–0.1 percent pyrite, mostly oxidized. Quartz schist is similar but contains less quartz (75–80 percent) and more muscovite (15–20 percent). Chemical analyses (Wypych and others, 2023) show that the unit is variably enriched in gold (Au), silver (Ag), arsenic (As), antimony (Sb), and vanadium (V). Magnetic susceptibility is uniformly low: 0.016–0.16 x 10^{-3} SI, with an average of 0.05 x 10^{-3} SI and a median of 0.04 x 10^{-3} SI.

pMfcsg SCHIST AND GNEISS OF FAIRBANKS-CHENA ASSEMBLAGE (PRE-MISSISSIPPIAN)—This is a composite unit that contains most of the Fairbanks-Chena rock types, although predominantly gneiss and schist. Based on rocks encountered in mapping, this unit is about 45 percent gneiss, 25 percent schist, 20 percent granitic rocks (primarily dikes?), and 10 percent others, including amphibolite, calc-silicate rocks (gneiss, hornfels, and skarn), pelitic hornfels, quartzite, and marble. However, in areas of good exposure (e.g., roadcuts), schist commonly comprises more than half of the rocks, and it may be considerably more abundant than suggested by weathered rock chip exposures. Of the gneiss, approximately 70 percent is paragneiss, 20 percent is orthogneiss (chiefly granite composition, but about one-fifth with diorite to granodiorite composition), and 10 percent is too altered to reliably classify. Of the schistose rocks, about 25 percent are quartz-rich, with more than 50 percent quartz. Most of these lithologies, except paragneiss and schist, were previously described.

Paragneiss is most commonly interspersed with schist or orthogneiss at a scale of 20–200 m. Paragneiss is predominantly black and white or tan to dark gray, weathering gray to dark brown. Grain sizes are typically 0.1–1.5 mm; gneissic bands are typically 0.5–2 mm wide, dominated by quartz and feldspar. Minerals present include: 50–70 percent quartz (0.1–2 mm, commonly with undulatory extinction, irregular grain boundaries, and forming thin, sub-millimeter layers), 15–30 percent plagioclase (0.2–2 mm, commonly twinned, forms bands, variably altered to sericite, approximately An_{15-30}), 0–10 percent alkali feldspar (0.3–2 mm, subhedral grains, little-altered), 3–15 percent biotite (0.2–2 mm, well-aligned in foliation, typically with trace to minor chlorite replacement), 0–5 percent

muscovite (0.1–0.3 mm, aligned parallel to biotite), 0–3 percent garnet (0.1–0.6 mm subhedral to euhedral grains, some partly replaced by chlorite), and minor amounts of chlorite and opaque minerals. In the central and northern part of the Richardson mining district map area, paragneiss is locally recrystallized, retaining gneissic banding, but with biotite possessing semi-random orientations. Such rocks can contain 2–3 percent sillimanite as randomly oriented fiber bundles, possibly as replacements of earlier kyanite. The sillimanite is, in turn, partly altered to sericite.

Schist is pale gray, silver, silver-pink, or white, weathering tan to brown with variable Fe staining; strong schistosity is typical. Schist is distinguished from paragneiss by higher mica abundance (25–65 percent) and a tendency to readily break into thin sheets. Micas typically form continuous sub-millimeter-thick layers. Grain size is typically 0.1–2 mm; rarely up to 5 mm. Schist typically contains 15–45 percent quartz (0.5–2 mm, typically with undulatory extinction and irregular grain boundaries), 10–25 percent plagioclase (0.5–2 mm, commonly twinned, forms bands, partly replaced by sericite and [or] clay, approximately An_{15-25}), 0–10 percent alkali feldspar (0.1–1.5 mm, some twinned, little-altered), 5–60 percent muscovite (subhedral, well-aligned grains), 5–30 percent biotite (0.1–1.5 mm, slightly to partially replaced by chlorite), 0–7 percent garnet (0.05–4 mm, subhedral to euhedral, locally skeletal). Other minerals variably present in small amounts include ilmenite, calcite, titanite, and clinozoisite. Quartz schist is similar but contains 50–70 percent quartz and less feldspar (2–10 percent). Samples within a kilometer of granitic intrusions can display partial recrystallization to a hornfels or granofels fabric, with semi-randomly oriented micas. Such rocks also contain 0–3 percent euhedral tourmaline and 0–20 percent sillimanite (commonly as fiber bundles with semi-random orientations). Some also contain anomalously abundant alkali feldspar (25–35 percent). The sillimanite presumably formed due to recrystallization at moderately low pressure, in some cases from the breakdown of muscovite + quartz to sillimanite + alkali feldspar.

Magnetic susceptibility of this unit is generally low, but variable (0.001–26 x 10^{-3} SI, with an average of 0.23 x 10^{-3} SI and a median of 0.11 x 10^{-3} SI), indicated by a mean value twice as high as the median. This variation reflects the wide variety of lithologies in the unit. This unit is correlated with similar rocks in the upper Chena area (Smith and others, 1994) and with the Fairbanks schist of Newberry and others (1996). Schist and quartz schist presumably represent more clay-rich protoliths and paragneiss represents more arkosic protoliths. The age is constrained by apparent intrusion of Mississippian granites, now orthogneiss.

Lake George Assemblage

The amphibolite-facies Lake George assemblage is interpreted to occupy the lowest structural level in the project area. The assemblage is composed of augen gneiss, orthogneiss, amphibolite,

paragneiss, schist, and quartz schist, with minor quartzite and rare marble. The metasedimentary lithologies may be the metamorphosed equivalents of the Neoproterozoic to Devonian passive margin strata of the Selwyn Basin that were deposited prior to the intrusion of Mississippian-Devonian granitic plutons. Orthogneiss and amphibolite mostly occur as layers concordant with foliation in the metasedimentary rocks. The rocks were metamorphosed to upper amphibolite facies (Newberry and Twelker, 2021) in the Early Cretaceous (Wildland, 2022) prior to rapidly cooling through the $^{40}Ar/^{39}Ar$ closure temperatures of multiple chronometers in the mid-Cretaceous (Pavlis and others, 1993; Dusel-Bacon and others, 2002; Jones and Benowitz, 2020; Naibert and others, 2020).

TrPzlu META-ULTRAMAFIC ROCKS OF THE LAKE GEORGE ASSEMBLAGE (TRIASSIC TO PALEOZOIC)—Unlike the Fairbanks-Chena-hosted meta-ultramafic rocks, this unit is strongly associated with, and locally surrounded by, amphibolite. The degree of intermixing is such that about 15 percent of this unit is amphibolite. These amphibolites do not possess trace element compositions characteristic of mid-ocean ridge basalt (Wypych and others, 2023), unlike the mafic rocks associated with the Seventymile ultramafic rocks (Dusel-Bacon and others, 2006; Buchanan, Wypych, and others, 2025). Aeromagnetic anomalies continuing beyond the surface extent of these rocks (Emond and MPX Geophysics Ltd., 2022) indicate that they are slabs within the host amphibolite-facies rocks. This is consistent with their amphibolite-facies mineralogy. The rocks vary considerably in texture and mineralogy. At or near margins they are strongly foliated and serpentinized (up to 95 percent serpentine), and away from body margins the minerals are coarser (typically 0.5–15 mm), possess semi-random orientations, and only include trace serpentine (1–3 percent). Magnetite content (0.5–5 percent) mostly varies with the abundance of serpentine + talc (low-Fe secondary minerals that force magnetite crystallization from the leftover iron). Sulfides (chiefly pentlandite and pyrrhotite) are ubiquitous, albeit at low concentrations (0.05–1 percent).

Roughly half of the ultramafic rocks in this unit contain 20 percent or less serpentine; elongate minerals in these rocks typically display semi-random orientations. These contain 15–75 percent olivine (0.1–7 mm, variably serpentinized, mostly Fo_{89-92}, but locally up to Fo_{95}); 0–10 percent (in one case 40 percent) enstatite (0.2–4 mm, most commonly anhedral relict grains mostly replaced by talc and [or] serpentine, mostly En_{83-93}); 0.5–25 percent anthophyllite (0.1–15 mm, mostly elongate grains, partly altered to talc or serpentine); 0.3–40 percent tremolite (0.3–10 mm, mostly elongate grains); 0–15 percent talc (0.05–1.5 mm, commonly with fine-grained magnetite); 1–20 percent (in one case 75 percent) Cr-chlorite (0.05–3 mm, variably aligned, with 0.5–4.5 weight percent Cr_2O_3); 0.7–2 percent magnetite (0.02–1.5 mm, subhedral to euhedral, commonly associated with serpentine and talc); 0–1 percent relict chromite (0.05–0.3 mm); and trace–one percent sulfide (pentlandite ± pyrrhotite). Rocks with abundant serpentine (60–95 percent) are generally finer grained (mostly 0.1–2 mm) and foliated; they notably

lack enstatite. In addition to serpentine, they contain 0–30 percent olivine (0.1–1 mm, commonly granulated, Fo_{82-87}), 0–5 percent anthophyllite (0.1–0.4 mm relicts, mostly replaced by talc or serpentine), 1–10 percent Cr-chlorite (0.05–0.5 mm), 1–15 percent tremolite (0.2–10 mm euhedral grains, commonly with semi-random orientations, unaltered), 0–15 percent talc (0.1–2 mm, subhedral to euhedral grains, unaltered), 2–5 percent magnetite (0.01–0.4 mm, anhedral to subhedral grains), trace–0.5 percent sulfide minerals (pentlandite, pyrrhotite, and [or] pyrite), and 0–8 percent carbonate minerals (dolomite or magnesite, 0.05–0.5 mm). These minerals and mineral compositions have been established with an electron microprobe as part of this study.

In addition to about 15 percent amphibolite (described as unit pMla), a rock type with its composition intermediate between ultramafic and mafic (less MgO and more CaO and Al_2O_3 than ultramafic) locally occurs. One example contains 45 percent tremolite (1–10 mm euhedral grains with semi-random orientations), 40 percent Cr-chlorite (0.3–1 mm, generally aligned), and 5 percent magnetite (0.1–0.7 mm, subhedral to euhedral grains). A second example is weakly foliated and contains 52 percent magnesio-hornblende (0.2–2 mm, some with tremolite cores), 10 percent tremolite (0.2–0.5 mm, partly replaces diopside), 15 percent diopside (0.05–0.3 mm relicts, partly altered to tremolite), 10 percent olivine (0.05–0.1 mm, relicts partly altered to hornblende or serpentine, Fo_{82-88}), 5 percent Cr-chlorite (0.05–0.2 mm), 5 percent serpentine (0.05–0.2 mm, alteration of olivine), with trace magnetite, pyrrhotite, and pentlandite. The latter rock might have an olivine clinopyroxenite protolith. The chlorite in these two rocks contains less Cr (0.1–1 weight percent) than that of the meta-ultramafic rocks. (Mineralogy and compositions determined by electron microprobe.) Magnetitic susceptibility in this unit is generally high, but variable (0.09–184 x 10^{-3} SI, with an average of 19 x 10^{-3} SI and a median of 17 x 10^{-3} SI). This is due both to the presence of less-magnetic amphibolite and to little-serpentinized rocks with low magnetite contents. It is unclear what these rocks should be correlated with. Seventymile terrane ultramafic is the traditional assignment (e.g., Wilson and others, 2015), but the association of this unit with amphibolites with arc-type trace element signatures suggests a different source. Correlated with unit MzPzum (meta-ultramafic and mafic rocks) of Werdon and others (2004).

MDag DIVIDE MOUNTAIN AUGEN GNEISS (EARLY MISSISSIPPIAN TO LATE DEVONIAN)—In the project area, this unit is approximately 85 percent granite orthogneiss, 5 percent other meta-igneous rocks (non-granite orthogneiss and minor amphibolite), 5 percent metasedimentary rocks (paragneiss and lesser schist), and 10 percent granitic dikes. Of the granite orthogneiss, approximately 75 percent displays 2–20 percent alkali feldspar megacrysts (“augen”), mostly 1–4 cm long, locally up to 6 cm. The unit is commonly white to light brown and has experienced minor to major weathering. Gneissic matrix is fine to coarse grained (0.1–3 mm); the micas commonly form foliation-parallel, mm-scale bands, which separate other felsic layers. Typical mineralogy for both

augen-bearing and augen-free granite gneiss includes 20–35 percent subhedral to anhedral alkali feldspar, 20–25 percent subhedral to anhedral plagioclase, 25–40 percent granoblastic quartz with irregular grain boundaries and common sub-grains, 5–15 percent biotite, and 3–15 percent muscovite. Plagioclase is slightly altered to sericite, and biotite is variably altered to chlorite. Minor minerals include up to 2 percent garnet, 3 percent clinozoisite, 5 percent chlorite, 3 percent tourmaline, 1 percent titanite, and trace opaque minerals, apatite, and zircon. The unit is characteristically non-magnetic to weakly magnetic, and is less magnetic than other orthogneiss units due to the abundance of granitic protolith. We interpret the minor metasedimentary rocks in this unit as former inclusions in, or screens between, megacrystic granite bodies. Magnetic susceptibility is mostly low (0.001–4.5 x 10^{-3} SI, with an average of 0.17 x 10^{-3} SI and a median of 0.09 x 10^{-3} SI), reflecting the predominance of granitic orthogneiss.

Dusel-Bason and others (2006) report U-Pb crystallization ages for 10 augen gneiss samples of 347 ± 5 to 371 ± 3 Ma. Twelker and others (2021a) observed the transition from minimally strained megacrystic granite into mylonitic augen orthogneiss in the eastern Tanacross Quadrangle, with U-Pb zircon ages of 367.6 ± 8.4 and 360.7 ± 8.7 Ma (samples 19SPR174 and 19ADW351C, respectively, in Wildland and others, 2021). Todd and others (2019) obtained a U-Pb zircon age of 355.0 ± 4.5 Ma from augen orthogneiss in the Divide Mountain area in the Tanacross D-1 Quadrangle. This unit correlates with the Divide Mountain augen gneiss of Wypych and others (2021), Twelker and others (2021a), and Naibert and others (2024).

MDla

AMPHIBOLITE OF THE LAKE GEORGE ASSEMBLAGE (EARLY MISSISSIPPIAN TO LATE DEVONIAN)—Mostly hornblende amphibolite with 10–20 percent hornblende quartz diorite to hornblende granodiorite orthogneiss, typically present as thin, 0.5–10-km-long lenses in unit MDlo (orthogneiss). The unit is dark green to gray, commonly weathers to brown, and is fine to medium grained; dominantly gneissic-textured rock. The predominant rock type is hornblende amphibolite (some partially retrograded to greenschist facies) with a 0.1–4 mm grain size. Typical mineralogy includes 45–75 percent hornblende (0.2–4 mm, subhedral, some with relict actinolite cores or late rims, some alteration to chlorite), 25–40 percent calcic plagioclase (0.1–1 mm subhedral grains, partly altered to sericite or clinozoisite, mostly An_{40-90}), 0–8 percent biotite (0.1–1 mm, typically with some alteration to chlorite), 0.3–3 percent chlorite (0.05–0.3 mm, partial replacement of hornblende and especially biotite), 0–10 percent garnet (0.1–4 mm, subhedral to euhedral), 0–10 percent diopside (0.1–0.3 mm, subhedral grains partly altered to actinolite), 0–4 percent clinozoisite-epidote (0.03–0.5 mm, subhedral to anhedral grains and clusters that mostly replace plagioclase), and 0.5–4 percent ilmenite + titanite + rutile. Quartz, magnetite, and pyrrhotite are variably present in small amounts. Hornblende quartz diorite orthogneiss is similar, but contains 5–10 percent quartz, less plagioclase, and

lacks diopside. Strongly retrograded samples contain up to 25 percent clinozoisite-epidote, 15 percent chlorite, and abundant secondary albite and actinolite.

Magnetic susceptibility is variable, but mostly moderate to high: 0.01–58 x 10^{-3} SI, with an average of 1.8 x 10^{-3} SI and a median of 0.38 x 10^{-3} SI. This amphibolite is correlated with Lake George assemblage amphibolite of Twelker and others (2021a) and Wypych and others (2021) and unit pMa in the Alaska Highway corridor (Solie and others, 2019). A U-Pb zircon age of 351.5 ± 4.3 Ma from correlative amphibolite was collected in the northeast Tanacross Quadrangle (Wypych and others, 2020).

MDlo ORTHOGNEISS OF THE LAKE GEORGE ASSEMBLAGE (EARLY MISSISSIPPIAN TO LATE DEVONIAN)—Based on samples collected during mapping, this unit consists of approximately 70 percent meta-igneous, 15 percent igneous (mostly granite and granodiorite dikes), and 15 percent metasedimentary rocks (chiefly paragneiss and schist, described with Lake George metasedimentary rocks [unit pMlms]). In many cases the meta-igneous and metasedimentary rocks seem interstratified. Of the meta-igneous rocks, approximately 10 percent are amphibolite (described in unit MDla), 5 percent are diorite or quartz diorite to tonalite; 10 percent are tonalite or trondhjemite orthogneiss; 15 percent are granodiorite orthogneiss, and 60 percent are granite orthogneiss. Of the latter, approximately 15 percent contain 5–30 mm alkali feldspar augen. In comparison, Divide Mountain augen gneiss unit MDag contains a much higher proportion of granite orthogneiss, typically with alkali feldspar augen.

Granite orthogneiss is mostly fine to medium grained, locally mylonitic or schistose, with a typical grain size of 0.1–4 mm; rare alkali feldspar augen are up to 40 mm. The rocks are tan, light brown, and gray, minimally to moderately weathered, and have experienced varying degrees of chloritic and sericitic alteration. Their mineralogy includes 25–35 percent alkali feldspar (mostly 0.2–4 mm, anhedral to subhedral grains, commonly twinned and inclusion-rich); 15–30 percent plagioclase (0.1–3 mm, subhedral grains with polysynthetic twinning and minor to significant sericite alteration); 30–40 percent quartz (0.1–4 mm, subhedral to anhedral dynamically recrystallized grains with undulose extinction); 0.5–12 percent biotite (0.05–1.5 mm, variably altered to chlorite); 0–10 percent muscovite (0.05–2.5 mm, subhedral grains); 0.3–9 percent chlorite (partial to nearly complete replacement of biotite and partial alteration of hornblende and garnet); 0–3 percent garnet (0.1–0.4 mm, subhedral to euhedral grains, some partly altered to chlorite); and (locally) 1–5 percent hornblende (0.1–2 mm, subhedral grains, partly chloritized). Biotite and muscovite commonly define the foliation. Accessory minerals variably present include pyrite, magnetite, apatite, zircon, epidote, ilmenite, allanite, and titanite. Sillimanite locally occurs, seemingly as a replacement of muscovite; relict (secondary?) andalusite occurs in one strongly retrograded sample.

Granodiorite orthogneiss is similar but contains less alkali feldspar (8–15 percent), with a grain size maximum of 3 mm, and more plagioclase (35–45 percent) and hornblende (5–10 percent). Secondary sericite and chlorite are present, but muscovite is absent. Tonalite, diorite, and quartz diorite orthogneiss basically lack alkali feldspar (0–2 percent) and contain significant (5–30 percent) hornblende, 45–60 percent plagioclase, 0–5 percent diopside, and 2–6 percent epidote in addition to 0–15 percent biotite. Titanite (1–3 percent) and apatite (0.5–1 percent) are ubiquitous. Trondhjemite is similar to tonalite orthogneiss but contains albite instead of plagioclase, and biotite is more strongly altered to chlorite. Diorite orthogneiss contains little quartz (1–3 percent) and is distinguished from amphibolite by its lower hornblende abundance (15–30 percent).

The unit generally has a low, but variable magnetic susceptibility (0.001–15 x 10^{-3} SI, average of 0.36 x 10^{-3} SI and median of 0.13 x 10^{-3} SI) as expressed by the considerably larger mean than median value. This is due to the wide variations in rock type present; amphibolite and non-granite orthogneiss commonly have higher values. A chloritized granite orthogneiss sample from this unit yielded a U-Pb zircon age of 362 ± 3 Ma (table 1; 22RN537; Buchanan, Gavel, and others, 2025). A chloritized granite orthogneiss from the western Tanacross Quadrangle yielded a U-Pb zircon crystallization age of 359.6 ± 1.3 Ma (Gavel and others, 2023). A leucogranite orthogneiss yielded a U-Pb zircon crystallization age of 370.6 ± 8.3 Ma (Wildland and others, 2021). This unit correlates to the Lake George orthogneiss of Twelker and others (2021a), Wypych and others (2021), and Naibert and others (2024).

pMlms METASEDIMENTARY ROCKS OF THE LAKE GEORGE ASSEMBLAGE (PRE-MISSISSIPPIAN)—A composite unit; based on field samples, it comprises approximately 5 percent granitic dikes, 5 percent meta-igneous rocks (amphibolite and orthogneiss), and 90 percent metasedimentary rocks. The latter include about 55 percent schist, 35 percent paragneiss, 5 percent quartzite, and 5 percent skarn + calc-silicate rocks. Thus, the rock types are the same as in unit pMlp (paragneiss), but schist is much more common than paragneiss. The lithologies are as described for unit pMlp. This unit has generally low, but variable magnetic susceptibility (0.005–10 x 10^{-3} SI, with an average of 0.22 x 10^{-3} SI and a median of 0.14 x 10^{-3} SI) due to the variety of rocks present; skarn, amphibolite, and non-granite orthogneiss are particularly variable. Orthogneiss within the metasediments suggests sediment deposition occurred prior to the Early Mississippian minimum age of unit MDlo. A detrital zircon sample along the Taylor Highway south of Taylor Mountain has a youngest U-Pb age population between 515 and 555 Ma (sample 16YTT021 in Jones and O'Sullivan, 2020), which suggests the sediment is Cambrian or younger. The composite unit likely comprises the metamorphic equivalents of at least parts of the Neoproterozoic through Devonian Selwyn Basin stratigraphy. This unit is correlated with Lake George metasedimentary rocks (pMlms) of Wypych and others (2021) and Naibert and others (2024).

pMlp PARAGNEISS OF THE LAKE GEORGE ASSEMBLAGE (PRE-MISSISSIPPIAN)—Based on samples collected during field mapping, the unit consists of about 75 percent metasedimentary rocks, 15 percent meta-igneous rocks (about one-quarter amphibolite, one-half granite orthogneiss, and one-quarter other orthogneiss), and 10 percent igneous rocks (mostly granitic dikes). The metasedimentary rocks are approximately 60 percent paragneiss, 25 percent schist and hornfelsed schist, 10 percent quartzite, and 5 percent skarn and calc-silicate rock. This unit contains the same lithologies as unit pMlms, but the metasedimentary rocks are dominantly paragneiss.

Paragneiss is predominantly black and white or tan to dark gray, weathering gray to dark brown. Grain sizes are typically 0.1–3 mm. Gneissic bands are typically 0.5–2 mm wide, dominated by quartz and feldspar; biotite occurs in bands that visibly define the gneissic texture. Minerals present include: 40–75 percent quartz (0.1–3 mm, commonly anhedral grains with undulatory extinction and irregular grain boundaries); 10–25 percent plagioclase (0.2–3 mm, commonly twinned, forms bands, variably altered to sericite); 0–10 percent alkali feldspar (0.2–0.6 mm, subhedral grains, little-altered); 5–15 percent biotite (0.2–2 mm, typically with trace to major chlorite replacement); 0–10 percent muscovite (0.1–2 mm); 0–10 percent garnet (0.05–1.5 mm subhedral grains, some partly replaced by chlorite); 0.5–15 percent sericite (slightly to strongly replaces plagioclase and to a smaller extent, alkali feldspar); 0–12 percent chlorite (trace to major replacement of biotite); and minor amounts of ilmenite, titanite, and apatite. Up to 8 percent staurolite (0.3–8 mm) is locally present. Samples from a discrete zone about 10–15 km northeast of Lake George variably contain aluminosilicates (both in paragneiss and schist). One sample was found to contain 0.5 percent relict kyanite (partly replaced by fine-grained muscovite), trace sillimanite, and 4 percent andalusite (1–4 mm, partly replaced by fine-grained muscovite). This sample preserves evidence of kyanite-stable peak metamorphism, followed by new aluminosilicate formation at lower pressures. Other samples from this area possess only 2–4 percent sillimanite (0.05–0.5 mm, mostly bundles of fibers); they might not have contained kyanite and instead formed sillimanite from breakdown of muscovite + quartz.

Schist in this unit contains more mica than paragneiss; the micas typically form continuous sub-millimeter thick layers. Grains are typically 0.1–3 mm; staurolite porphyroblasts are up to 7 mm. This schist typically contains 20–55 percent quartz (0.1–3 mm, typically with undulatory extinction and irregular grain boundaries); 5–35 percent plagioclase (0.1–3 mm, commonly twinned, forms bands, partly replaced by sericite and [or] clay); 0–7 percent alkali feldspar (0.1–3 mm, some twinned, little-altered); 5–60 percent muscovite (0.1–3 mm, subhedral to euhedral); 5–30 percent biotite (0.1–3 mm, slightly to moderately replaced by chlorite); 0–12 percent garnet (0.05–3 mm, subhedral to euhedral); 0.2–4 percent sericite (partial alteration of plagioclase); 0.3–5 percent chlorite (slight to significant alteration of biotite); and 0–2 percent tourmaline (0.05–0.5 mm, euhedral grains). Other minerals variably present in small amounts include ilmenite, rutile, apatite,

and zircon. Quartz schist is similar and relatively rare; it contains more quartz (60–70 percent) and less total feldspar (5–15 percent). One schist sample from 10 km northeast of Lake George was found to contain 2 percent kyanite as 0.5–5 mm elongate grains partly replaced by muscovite. Sillimanite is more common; about half the occurrences are near contacts with granitic bodies and may represent contact metamorphic effects. The other half are from the same region 10–15 km northeast of Lake George that contains sillimanite-bearing paragneiss. The contact-related rocks contain more (5–15 percent) and coarser (up to 1.5 mm) sillimanite. Both types occur with significant alkali feldspar (5–20 percent) that may be due to muscovite destruction.

Rocks identified as hornfels (or granofels) possess micas with semi-random orientations and appear to have both paragneiss and schist protoliths. Most are located adjacent to granitic intrusions; one sample is from the aluminosilicate zone northeast of Lake George. One sample contains 0.5–3.5 mm randomly oriented andalusite porphyroblasts; the others contain 10–15 percent sillimanite, commonly as 0.5–1.5 mm randomly oriented prisms. Associated minerals include cummingtonite, anthophyllite, and cordierite, all confirmed by microprobe.

Quartzite is gray to pale green and weathers light tan to orange; very fine to fine grained (0.05–0.5 mm); weakly foliated; and is composed of 85–95 percent quartz (anhedral, sometimes parted by thin mica layers); 1–10 percent muscovite (fine grained, often as single-crystal layers); 1–5 percent biotite (slightly to partly altered to chlorite); 5–10 percent plagioclase (anhedral, usually untwinned grains, locally stretched, partly altered to sericite); 0–2 percent garnet (subhedral to euhedral grains, some slightly chloritized); 0.3–1.5 percent chlorite (variably replaces biotite and garnet); and variably trace amounts of calcite, alkali feldspar, and pyrite.

Skarn is a contact metamorphic rock composed mostly of calc-silicates, thought to be at least in part derived by reactions between igneous-derived fluids and carbonate-rich rocks. In this region, skarn is typically fine to coarse grained (0.1–5 mm), medium to dark green and brown to black colored. Skarn in the map area is dominated by relatively Fe-rich (Hd_{40-80}), distinctly green pleochroic clinopyroxene (20–75 percent), and calcic (An_{80-95}) plagioclase (5–55 percent), with lesser garnet (15–25 percent), hornblende (0–10 percent, typically a replacement of pyroxene), quartz (0–8 percent), and epidote (1–3 percent, replaces garnet and plagioclase). Titanite (0.5–3 percent), apatite (0.2–1 percent), and sulfide minerals (0.3–2 percent) are also present. Chemical analyses (Wypych and others, 2023) show that these rocks are variably anomalous in copper (Cu), zinc (Zn), lead (Pb), As, Ag, Au, W, and (or) tin (Sn). These rocks are present within 600 m of known granitic bodies. Rocks farther away (>1 km) possess more distinct mineralogical banding and generally paler-colored (more Fe-poor) minerals. They also commonly possess more quartz (10–55 percent) and lack hornblende and visible sulfide minerals. These calc-silicate

rocks may represent more siliceous and less calcareous protoliths and (or) rocks that have been less altered by igneous-related hydrothermal fluids.

Magnetic susceptibility of this unit is generally low, but variable: 0.001–15 x 10^{-3} SI, with an average of 0.29 x 10^{-3} SI and a median of 0.1 x 10^{-3} SI. This is due in part to the variety of rock type present; additionally, hornfels, skarn, and paragneiss in this unit show considerable variation. Orthogneiss and augen gneiss bodies within the unit suggest sediment deposition occurred prior to the Early Mississippian minimum age of units MDag and MDlo. An anthophyllite granofels sample of uncertain protolith in this unit (22Z237) yielded a U-Pb crystallization age of 365 ± 2 Ma (table 1; Buchanan, Gavel, and others, 2025). Correlated with the Scottie Creek Formation in Canada (Yukon Geological Survey, 2019) and Lake George paragneiss (pMlp) of Naibert and others (2024).

pMlrp RECRYSTALLIZED PARAGNEISS OF THE LAKE GEORGE ASSEMBLAGE (PRE-MISSISSIPPIAN)—This unit occurs in the northern half of the Richardson mining district map area. Based on data from industry drilling (Graham, 2002), it structurally underlies Fairbanks-Chena units. Based on samples collected during field mapping, it consists of approximately 60 percent paragneiss, 15 percent schist, 20 percent granitic rock, and 5 percent other lithologies, including amphibolite, orthogneiss, quartzite, and ambiguous gneiss. This unit differs from typical Lake George paragneiss seen to the east. It is partly recrystallized, with semi-randomly oriented micas; it commonly contains sillimanite, and it contains a high abundance of granitic dikes. In contrast, kyanite is a common aluminosilicate seen to the east. Most likely this paragneiss has undergone recrystallization during a relatively high-temperature, moderate-pressure fluid-influx event. Based on the variable presence of either muscovite or alkali feldspar with sillimanite, sillimanite content is probably due to a high-aluminum (Al) protolith, and some is due to the reaction quartz + muscovite = sillimanite + orthoclase. Nearly all of the thin sections examined (20) contained sillimanite; it is likely to be at least commonly present in the rocks, even if not obvious in hand specimen.

Paragneiss is predominantly black and white or tan to dark gray, weathering gray to dark brown. Grain sizes are typically 0.1–2.5 mm. Gneissic bands are typically 0.5–2 mm wide, dominated by quartz and feldspar; biotite occurs in bands, but grains display semi-random orientations. Minerals present include: 45–75 percent quartz (0.1–2.5 mm, commonly anhedral grains with undulatory extinction and irregular grain boundaries); 10–35 percent plagioclase (0.2–2 mm, commonly twinned, forms bands, variably altered to sericite, approximately An_{20-30}); 0–8 percent alkali feldspar (0.2–1.5 mm, subhedral grains, little-altered); 6–20 percent biotite (0.2–2 mm, poorly aligned, typically with trace to minor chlorite replacement); 0–10 percent sillimanite (mostly bundles of 0.05–0.15 mm fibers, with rare 0.1–0.6 mm prismatic grains with semi-random orientations); 0–8 percent muscovite (0.1–0.4 mm, poorly aligned); 0–0.5 percent garnet (0.05–0.2 mm subhedral

grains, some partly replaced by chlorite); 1–3 percent sericite (partly replaces plagioclase and sillimanite); and minor amounts of chlorite, apatite, and opaque minerals. Hydrothermally altered versions contain up to 20 percent sericite as a near-complete replacement of plagioclase and—especially—sillimanite; pyrite and tourmaline are common associates.

Schist in this unit contains more mica than the paragneiss. The micas commonly display partial recrystallization with semi-random as well as well-aligned crystals present. Due to this partial recrystallization, this schist commonly does not break into thin sheets; however, the micas typically form continuous sub-millimeter thick layers. Grain size is typically 0.1–3 mm. This schist typically contains 20–60 percent quartz (0.1–3 mm, typically with undulatory extinction and irregular grain boundaries); 5–30 percent plagioclase (0.1–3 mm, commonly twinned, forms bands, partly replaced by sericite and [or] clay, approximately An_{20-30}); 0–5 percent alkali feldspar (0.1–1 mm, some twinned, little-altered); 5–35 percent muscovite (subhedral, variably aligned grains); 0–18 percent sillimanite (mostly bundles of 0.05–0.15 mm fibers, with rare 0.2–0.3 mm prismatic grains with semi-random orientations, partly altered to sericite); 20–30 percent biotite (0.1–3 mm, variably aligned, slightly to moderately replaced by chlorite); 0–0.5 percent garnet (0.05–0.3 mm, subhedral to euhedral); 0.5–2 percent sericite (partial alteration of plagioclase and sillimanite); and 0.3–4 percent chlorite (as slight to significant alteration of biotite). Other minerals variably present in small amounts include ilmenite, apatite, and zircon. Where hydrothermally altered, contains 8–20 percent sericite replacing plagioclase and—especially—sillimanite, commonly with pyrite.

This unit has a nearly uniform low magnetic susceptibility (0.001–1.2 x 10^{-3} SI, with an average of 0.14 x 10^{-3} SI and a median of 0.13 x 10^{-3} SI); all the component rock types have low magnetite contents. It is broadly correlated with Lake George paragneiss in the Tanacross Quadrangle (Naibert and others, 2024) and with the Scottie Creek Formation in Canada (Yukon Geological Survey, 2019).

pMlmpg MIGMATITIC PARAGNEISS OF THE LAKE GEORGE ASSEMBLAGE (PRE-MISSISSIPPIAN)—At the lowest structural levels, particularly in the Shaw Creek valley, recrystallized paragneiss (unit pMlrp) exhibits variably developed migmatitic texture (fig. 1A). In this mixed rock, well-foliated biotite-feldspar-quartz paragneiss melanosomes form irregular to rounded bodies, typically 1–20 cm in diameter, which have somewhat diffuse margins. The melanosome is surrounded by an interconnected network of unfoliated, equigranular, fine-grained leucosome comprising quartz, alkali feldspar-plagioclase, and several percent biotite. The overall appearance of the rock closely resembles leopard print. At the best exposure of this unit (a quarry at mile 9.5 of the Pogo Mine Road), some parts of the outcrop could be described as gneissic xenoliths within granitic dike rock (fig. 1B). Graham (2002) analyzed migmatite from drill core at the Bald Knob prospect, finding that

the leucosome has a bulk composition of an igneous rock, but that the composition is not consistent with partial melting of the local gneiss at the pressure and temperature estimated for the area. On this basis, Graham (2002) concludes that the rocks are injection migmatites, with the granitic leucosome sourced elsewhere and emplaced under high-pressure, ductile conditions. Magnetic susceptibility is uniformly low: 0–0.7 x 10^{-3} SI, with an average of 0.15 x 10^{-3} SI and a median of 0.14 x 10^{-3} SI.

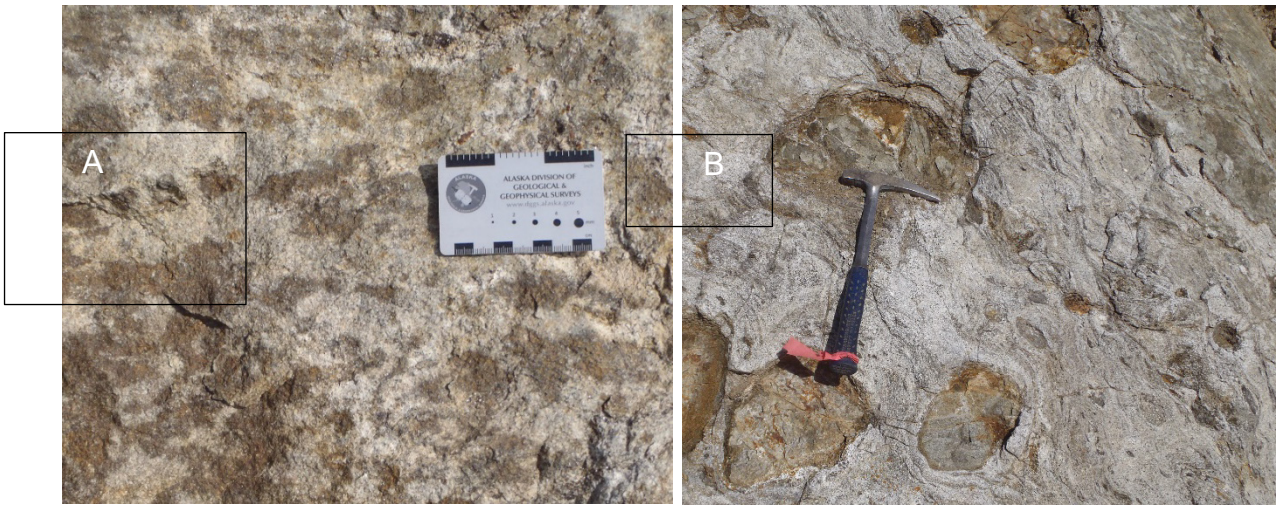

Figure 1. A. Migmatitic paragneiss texture exposed in a quarry along the Pogo Mine Road. The dark brown is biotite-rich paragneiss (melanosome), which is surrounded by quartz-alkali feldspar-plagioclase (leucosome). **B.** Leucosome-rich endmember, where rounded melanosome bodies more closely resemble xenoliths within granitic dikes.

MZlu

LAKE GEORGE ASSEMBLAGE, UNDIVIDED (MISSISSIPPIAN to PROTEROZOIC)—This unit is mapped in areas where Lake George assemblage rocks are suspected based on nearby occurrences, but rock exposures are not known, typically due to extensive loess, aeolian sand, or soil cover. Any or all of the various Lake George lithologies could be present at depth in such areas.

Table 1. Geochronology samples in the Mount Harper-Richardson project area.

Age Type	Sample ID	Age (Ma)	2σ Age Error (Ma)	Notes	Reference	Latitude (NAD83)	Longitude (NAD83)
Muscovite $^{40}Ar/^{39}Ar$	22ADW145	110.32	0.06	plateau age	Truskowski and others, 2025	63.8864	-144.3745
Hornblende $^{40}Ar/^{39}Ar$	22ADW204	108.77	0.06	weighted mean age	Truskowski and others, 2025	64.1448	-144.1311
Hornblende $^{40}Ar/^{39}Ar$	22RN093	192.4	0.4	weighted mean age	Truskowski and others, 2025	64.3829	-143.1788
Hornblende $^{40}Ar/^{39}Ar$	22Z189	114.8	0.6	plateau age	Truskowski and others, 2025	63.8441	-144.1734
Muscovite $^{40}Ar/^{39}Ar$	22SNF048	165.3	0.8	weighted mean age	Truskowski and others, 2025	64.4553	-143.2458
Muscovite $^{40}Ar/^{39}Ar$	22RN065	128.3	0.8	weighted mean age	Truskowski and others, 2025	64.0786	-143.3766
Muscovite $^{40}Ar/^{39}Ar$	22Z386	127.7	1	weighted mean	Truskowski and others, 2025	64.4814	-145.4295
Muscovite $^{40}Ar/^{39}Ar$	22NJB142	133.9	1	weighted mean age	Truskowski and others, 2025	64.2030	-145.7555
Muscovite $^{40}Ar/^{39}Ar$	22TJN044	154	1	weighted mean age	Truskowski and others, 2025	64.1826	-143.4804
Hornblende $^{40}Ar/^{39}Ar$	22MMG174	140.2	1	weighted mean age	Truskowski and others, 2025	64.1584	-145.8548
Hornblende $^{40}Ar/^{39}Ar$	22RN184	73.3	0.8	weighted mean age	Truskowski and others, 2025	64.1560	-145.1488
Muscovite $^{40}Ar/^{39}Ar$	22IPM084	171.7	1.4	weighted mean age	Truskowski and others, 2025	64.1679	-143.3099
Sericite $^{40}Ar/^{39}Ar$	22MLB313	100.6	1	weighted mean age	Truskowski and others, 2025	64.4641	-146.1903
Hornblende $^{40}Ar/^{39}Ar$	22RN279	122.3	1	weighted mean age	Truskowski and others, 2025	63.9033	-144.2989
Muscovite $^{40}Ar/^{39}Ar$	22IPM054	186.4	1.2	weighted mean age	Truskowski and others, 2025	64.4680	-143.4974
Muscovite $^{40}Ar/^{39}Ar$	22IPM137	100.07	0.1	weighted mean age	Truskowski and others, 2025	63.8443	-144.1734
Hornblende $^{40}Ar/^{39}Ar$	22TJN154	109.51	0.12	plateau age	Truskowski and others, 2025	64.2399	-143.8932
Muscovite $^{40}Ar/^{39}Ar$	22ADW224	111.39	0.28	weighted mean age	Truskowski and others, 2025	64.1630	-144.5014
Muscovite $^{40}Ar/^{39}Ar$	22IPM062	227.1	1.4	weighted mean age	Truskowski and others, 2025	64.4270	-143.3650
Muscovite $^{40}Ar/^{39}Ar$	22TJN113	119.4	1.4	weighted mean age	Truskowski and others, 2025	64.0119	-143.3498
Hornblende $^{40}Ar/^{39}Ar$	22MMG188	113	8	plateau age	Truskowski and others, 2025	64.0303	-144.5930
Sericite $^{40}Ar/^{39}Ar$	22Z405	113.8	1.2	weighted mean	Truskowski and others, 2025	64.2040	-145.5286
Muscovite $^{40}Ar/^{39}Ar$	22ADW217	115.95	0.26	weighted mean age	Truskowski and others, 2025	64.0479	-144.5530
Muscovite $^{40}Ar/^{39}Ar$	22RN385	106.08	0.32	weighted mean age	Truskowski and others, 2025	64.1060	-144.8245
Zircon U-Pb	22IPM013	190.20	2.10		Buchanan, Gavel, and others, 2025	64.1779	-142.4302
Zircon U-Pb	22TJN212	96.37	0.39		Buchanan, Gavel, and others, 2025	64.2212	-144.4357
Zircon U-Pb	22ET061	107.47	0.51		Buchanan, Gavel, and others, 2025	64.3202	-143.5838

Age Type	Sample ID	Age (Ma)	2σ Age Error (Ma)	Notes	Reference	Latitude (NAD83)	Longitude (NAD83)
Zircon U-Pb	22ET125	108.51	0.73		Buchanan, Gavel, and others, 2025	64.0256	-143.5891
Zircon U-Pb	22SNF222	98.57	0.55		Buchanan, Gavel, and others, 2025	64.2887	-145.4322
Zircon U-Pb	18TJN029	90.32	0.71		Buchanan, Gavel, and others, 2025	64.3367	-146.5329
Zircon U-Pb	22Z338	96.54	0.49		Buchanan, Gavel, and others, 2025	64.2406	-144.3796
Zircon U-Pb	22Z339	97.13	0.49		Buchanan, Gavel, and others, 2025	64.2406	-144.3799
Zircon U-Pb	22ET069	108.10	0.80		Buchanan, Gavel, and others, 2025	64.3262	-143.5465
Zircon U-Pb	22TJN033	66.15	0.84		Buchanan, Gavel, and others, 2025	63.8524	-142.3325
Zircon U-Pb	22IPM145	93.10	0.80		Buchanan, Gavel, and others, 2025	63.7770	-144.1048
Zircon U-Pb	22MLB313	93.12	0.87		Buchanan, Gavel, and others, 2025	64.4641	-146.1903
Zircon U-Pb	22TJN148	103.9	1.4		Buchanan, Gavel, and others, 2025	64.1507	-144.1702
Zircon U-Pb	22Z162	86.4	1.4		Buchanan, Gavel, and others, 2025	64.2410	-143.6834
Zircon U-Pb	22Z212	104.5	1.2		Buchanan, Gavel, and others, 2025	63.9728	-144.3372
Zircon U-Pb	22Z229	101.53	1.42		Buchanan, Gavel, and others, 2025	64.0255	-144.0404
Zircon U-Pb	22RN537	361.7	2.7		Buchanan, Gavel, and others, 2025	64.4102	-145.2633
Zircon U-Pb	22MMG077	107.63	0.54		Buchanan, Gavel, and others, 2025	64.4428	-143.6436
Zircon U-Pb	22NJB066	109.31	0.57		Buchanan, Gavel, and others, 2025	64.0318	-143.5911
Zircon U-Pb	22AW084	89.57	0.63		Buchanan, Gavel, and others, 2025	64.1461	-145.0766
Zircon U-Pb	22RN487	95.17	0.71		Buchanan, Gavel, and others, 2025	64.2819	-145.4482
Zircon U-Pb	22RN119			105-115 Ma; no preferred age	Buchanan, Gavel, and others, 2025	64.2209	-143.2141
Zircon U-Pb	22MMG196	95.10	1.70	85-105 Ma; no preferred age	Buchanan, Gavel, and others, 2025	64.2353	-144.0636
Zircon U-Pb	22RN028			no preferred age	Buchanan, Gavel, and others, 2025	63.8982	-142.0198
Zircon U-Pb	22ADW256	62.53	0.47		Buchanan, Gavel, and others, 2025	64.3576	-145.0735
Zircon U-Pb	22TJN285	56.61	0.4		Buchanan, Gavel, and others, 2025	64.0861	-145.1898
Zircon U-Pb	22RN229	106.9	1.5		Buchanan, Gavel, and others, 2025	63.7972	-144.0413
Zircon U-Pb	22Z237	364.9	2.3		Buchanan, Gavel, and others, 2025	64.0137	-144.0794
Zircon U-Pb	22Z276	103.99	0.79		Buchanan, Gavel, and others, 2025	64.1078	-144.2769
Zircon U-Pb	22Z299	90.79	0.75		Buchanan, Gavel, and others, 2025	64.2464	-144.8641
Zircon U-Pb	22SNF023	358.30	3.80		Buchanan, Gavel, and others, 2025	64.2643	-143.5266

Table 2. Magnetic susceptibility by map unit (all values are x 10^{-3} SI).

Label	Unit name	Mean	Median	Min	Max	Count
PEfp	Paleogene felsic porphyry	0.1	0.07	0.007	1.2	21
PEm	Paleogene mafic intrusions	0.36	0.36	0.23	0.47	1
lKfv	Felsic volcanic rocks of Middle Fork volcanic complex	6.9	8.08	0.06	17	30
lKpg	Porphyritic granite of Middle Fork volcanic complex	5.7	6.09	0.102	15	16
lKag	Alkaline gabbro of Taurus suite	0.37	0.45	0.04	0.7	4
lKm	Quartz monzodiorite of Taurus suite	0.24	0.2	0.033	0.6	9
lKgd	Granodiorite of Taurus suite	1.8	1.12	0.059	7.0	6
Kfsg	Granite of Fairbanks-Salcha suite	0.11	0.07	0.001	0.9	109
Kfsgd	Granodiorite of Fairbanks-Salcha suite	0.16	0.14	0.019	1.2	27
Kfsp	Porphyry of Fairbanks-Salcha suite	0.35	0.1	0.001	5.2	39
Kfsqd	Quartz diorite of Fairbanks-Salcha suite	0.57	0.34	0.026	5.2	26
Kfsmg	White mica-bearing granite of Fairbanks-Salcha suite	0.08	0.04	0.002	0.5	42
Kgt	Tonalite of Gardiner suite	7.5	7.2	2.3	13	3
Khg	Granite of Harper suite	1.1	0.14	0.001	47	326
Khgd	Granodiorite of Harper suite	7.2	6.47	0.02	31	87
Khgp	Granite porphyry of Harper suite	2.11	0.23	0.015	13	18
Pkmb	Metabasite of Klondike assemblage	0.28	0.30	0.011	1.6	15
Pks	Schist of Klondike assemblage	0.15	0.10	0.003	1.1	28
MDnm	Metabasite of Nasina assemblage	1.79	0.28	0.071	39	10
MDnms	Metasedimentary rocks of Nasina assemblage	0.12	0.06	0.004	3.8	73
MDfms	Metasedimentary rocks of Fortymile River assemblage	0.22	0.15	0.004	3.6	116
MDfp	Paragneiss of Fortymile River assemblage	0.17	0.13	0.010	1.5	32
MDfa	Amphibolite of Fortymile River assemblage	1.23	0.47	0.038	18	8
MDfo	Orthogneiss of Fortymile River assemblage	0.3	0.23	0.002	3.6	37
MDbms	Metasedimentary rocks of Butte assemblage	0.15	0.12	0.023	0.8	22
TRPzfcu	Fairbanks-Chena meta-ultramafic rocks	22	20	0.021	152	27
pMfca	Amphibolite of Fairbanks-Chena assemblage	4.42	0.46	0.014	80	19
MDfco	Orthogneiss of Fairbanks-Chena assemblage	0.49	0.11	0	13	67

Label	Unit name	Mean	Median	Min	Max	Count
pMfccs	Calc-silicate gneiss of Fairbanks-Chena assemblage	0.24	0.24	0.022	0.65	19
pMfcg	Graphitic rocks of Fairbanks-Chena assemblage	0.14	0.12	0.002	0.48	10
pMfcm	Marble of Fairbanks-Chena assemblage	0.17	0.15	0.112	0.29	4
pMfcq	Quartzite of Fairbanks-Chena assemblage (Richardson map)	0.55	0.10	0	23	45
pMfcsg	Schist & gneiss of Fairbanks-Chena assemblage	0.23	0.11	0	26	247
ŦrPzlu	Lake George meta-ultramafic rocks	19	17	0.091	184	53
MDag	Divide Mountain augen gneiss	0.17	0.09	0.001	4.5	273
MDla	Amphibolite of Lake George assemblage	1.81	0.38	0.01	58	64
MDlo	Orthogneiss of Lake George assemblage	0.36	0.13	0.001	15	543
pMlms	Metasedimentary rocks of Lake George assemblage	0.22	0.14	0.005	10	104
pMlp	Paragneiss of Lake George assemblage	0.29	0.10	0.0005	15	397
done	Recrystallized Paragneiss of Lake George assemblage	0.14	0.13	0	1.2	178
pMlmpg	Migmatitic paragneiss of Lake George assemblage	0.15	0.14	0.002	0.7	58

ACKNOWLEDGMENTS

We would like to thank Sean P. Regan and Melanie B. Werdon for thorough and constructive reviews of the geologic maps and accompanying map unit descriptions in this pamphlet. We gratefully acknowledge Doyon, Limited for access to its lands within the study area.

Work in the Richardson mining district benefited greatly from reports and information generated by exploration companies, current and former, that have worked in the area over the past three decades. In particular, we acknowledge the assistance of Dennis McDowell and Great American Minerals Exploration, INC (GAME), Peter Grieve and Koza Limited, Bill Cronk and Northern Empire Resources Corp., Phil St. George and Millrock Resources, and David Wright of Aurora Resource Exploration.

This project was jointly funded by the State of Alaska and the U.S. Geological Survey Earth Mapping Resources Initiative (Earth MRI) through cooperative agreement G22AC00288. The views and conclusions contained in this document are those of the authors and should not be interpreted as representing the opinions or policies of the U.S. Geological Survey. Mention of trade names or commercial products does not constitute their endorsement by the U.S. Geological Survey.

REFERENCES

Bacon, C.R., Dusel-Bacon, Cynthia, Aleinikoff, J.N., and Slack, J.F., 2014, The Late Cretaceous Middle Fork caldera, its resurgent intrusion, and enduring landscape stability in east-central Alaska: Geosphere, v. 10, p. 1432–1455. https://doi.org/10.1130/GES01037.1

Beranek, L.P., and Mortensen, J.K., 2011, The timing and provenance record of the Late Permian Klondike orogeny in northwestern Canada and arc-continent collision along western North America: Tectonics, v. 30, TC5017. https://doi.org/10.1029/2010TC002849

Buchanan, J.W., Gavel, M.M., Wildland, A.D., and Newberry, R.J., 2025, LA-ICP-MS uranium lead geochronologic data of zircon from igneous and meta-igneous rocks in the Mount Harper project area, Eagle, Tanacross, Mount Hayes, and Big Delta quadrangles, Alaska: Alaska Division of Geological & Geophysical Surveys Report of Investigation 2025-14. https://doi.org/10.14509/31552

Buchanan, J.W., Wypych, Alicja, Barrera, M.L., Biegel, J.M., Gavel, M.M., Harvey, D.A., Ketcham, R.A., Muller, I.P., Naibert, T.J., Newberry, R.J., Regan, S.P., Szumigala, D.J., Twelker, Evan, and Wildland, A.D., 2025, Geochemical data from samples collected in 2023 for the Chena and Mount Harper projects, Big Delta, Circle, Fairbanks, and Eagle quadrangles, Alaska: Alaska Division of Geological & Geophysical Surveys Raw Data File 2024-2, 5 p. https://doi.org/10.14509/31123

Burns, L.E., Graham, G.R.C., Barefoot, J.D., Woods, Rebecca-Ellen, Dighem, and WGM, Inc., 2020, Richardson electromagnetic and magnetic airborne geophysical survey data compilation: Alaska Division of Geological & Geophysical Surveys Geophysical Report 2019-22, 12 p. https://doi.org/10.14509/30263

Colpron, Maurice, Nelson, J.L., and Murphy, D.C., 2006, A tectonostratigraphic framework for the pericratonic terranes of the northern Canadian Cordillera, *in* Colpron, Maurice, and Nelson, J.L., eds., Paleozoic evolution and metallogeny of pericratonic terranes at the ancient Pacific margin of North America, Canadian and Alaskan Cordillera: Geological Association of Canada Special Paper, v. 45, p. 1–23.

Day, W.C., Aleinikoff, J.N., Roberts, Paul, Smith, Moira, Gamble, B.M., Henning, M.W., Gough, L.P., and Morath, L.C., 2003, Geologic map of the Big Delta B-2 Quadrangle, east-central Alaska: U.S. Geological Survey Geologic Investigations Series Map 2788, 1 sheet, scale 1:63,360.

Day, W.C., O'Neill, J.M., Aleinikoff, J.N., Green, G.N., Saltus, R.W., and Gough, L.P., 2007, Geologic map of the Big Delta B-1 Quadrangle, east-central Alaska: U.S. Geological Survey Scientific Investigations Map 2975, 1 sheet, scale 1:63,360.

Day, W.C., O'Neill, J.M., Dusel-Bacon, Cynthia, Aleinikoff, J.N., and Siron, C.R., 2014, Geologic map of the Kechumstuk fault zone in the Mount Veta area, Fortymile mining district, east-central Alaska: U.S. Geological Survey Scientific Investigations Map 3291, 1 sheet, scale 1:63,360.

Dusel-Bacon, Cynthia, Aleinikoff, J.N., Day, W.C., and Mortensen, J.K., 2015, Mesozoic magmatism and timing of epigenetic Pb-Zn-Ag mineralization in the western Fortymile mining district, east-central Alaska: Zircon U-Pb geochronology, whole-rock geochemistry, and Pb isotopes: Geosphere, v. 11, no. 3, p. 786–822. https://doi.org/10.1130/GES01092.1

Dusel-Bacon, Cynthia, and Harris, A.G., 2003, New occurrences of late Paleozoic and Triassic fossils from the Seventymile and Yukon-Tanana Terranes, east-central Alaska, with comments on previously published occurrences in the same area: Studies by the U.S. Geological Survey in Alaska, 2001: U.S. Geological Survey Professional Paper 1678, p. 5–30.

Dusel-Bacon, Cynthia, Hopkins, M.J., Mortensen, J.K., Dashevsky, S.S., Bressler, J.R., and Day, W.C., 2006, Paleozoic tectonic and metallogenic evolution of the pericratonic rocks of east-central Alaska and adjacent Yukon Territory, *in* Colpron, Maurice, and Nelson, J.L., eds., Paleozoic evolution and metallogeny of pericratonic terranes at the ancient Pacific margin of North America, Canadian and Alaskan Cordillera: Geological Association of Canada Special Paper 45, p. 25–74.

Dusel-Bacon, Cynthia, Lanphere, M.A., Sharp, W.D., Layer, P.W., and Hansen, V.L., 2002, Mesozoic thermal history and timing of structural events for the Yukon-Tanana Upland, east-central Alaska: $^{40}Ar/^{39}Ar$ data from metamorphic and plutonic rocks: Canadian Journal of Earth Sciences, v. 39, p. 1,013–1,051. https://doi.org/10.1139/e02-018

Dusel-Bacon, Cynthia, Slack, J.F., Aleinikoff, J.N., and Mortensen, J.K., 2009, Mesozoic magmatism and base-metal mineralization in the Fortymile mining district, eastern Alaska—Initial results of petrographic, geochemical, and isotopic studies in the Mount Veta area, *in* Haeussler, P.J., and Galloway, J.P. eds., Studies by the U.S. Geological Survey in Alaska, 2007: U.S. Geological Survey Professional Paper 1760-A, 42 p. http://pubs.usgs.gov/pp/1760/a/

Dusel-Bacon, Cynthia, Wooden, J.L., and Hopkins, M.J., 2004, U-Pb zircon and geochemical evidence for bimodal mid-Paleozoic magmatism and syngenetic base-metal mineralization in the Yukon-Tanana terrane, Alaska: Geological Society of America Bulletin, v. 116, p. 989–1015.

Dusel-Bacon, Cynthia, Wooden, J.L., and Layer, P.W., 2003, A Cretaceous ion-microprobe U-Pb zircon age for the West Point orthogneiss: Evidence for another gneiss dome in the Yukon-Tanana Upland, *in* Galloway, J.P., ed., Studies by the U.S. Geological Survey in Alaska, 2001: U.S. Geological Survey Professional Paper 1678, p. 41–60.

Emond, A.M., and MPX Geophysics Ltd., 2022, Tanana River and Big Delta airborne magnetic and radiometric survey: Alaska Division of Geological & Geophysical Surveys Geophysical Report 2022-1, 4 p. https://doi.org/10.14509/30899

Foster, H.L., compiler, 1976, Geologic map of the Eagle Quadrangle, Alaska: U.S. Geological Survey Miscellaneous Investigations Series Map 922, 1 sheet, scale 1:250,000.

Gavel, M.M., Regan, S.P., Holland, Mark, Wildland, A.D., Wypych, Alicja, Naibert, T.J., and Twelker, Evan, 2023, U-Pb zircon geochronology of bedrock samples collected in the Eagle and Tanacross quadrangles, eastern Alaska: Alaska Division of Geological & Geophysical Surveys Preliminary Interpretive Report 2023-2, 38 p. https://doi.org/10.14509/31013

Graham, G.E., 2002, Geology and gold mineralization of the Richardson district, east-central Alaska: unpublished MS thesis, University of Alaska, Fairbanks, Alaska, 150 p.

Holm-Denoma, C.S., Sicard, K.R., and Twelker, Evan, 2020, U-Pb geochronology of igneous and detrital zircon samples from the Tok River area, eastern Alaska Range, and Talkeetna Mountains, Alaska: Alaska Division of Geological & Geophysical Surveys Raw Data File 2020-3, 20 p. https://doi.org/10.14509/30439

Hunter, Ed, and Giroux, Gary, 2014, Technical Report on the LMS Gold project, Goodpaster Mining District, Alaska, 60 p. NI 43-101 technical report, accessed June 1, 2017.

Jones, J.V., III, and Benowitz, J.A., 2020, $^{40}Ar/^{39}Ar$ isotopic data and ages for rocks from the Yukon-Tanana Upland of eastern Alaska and the northern Aleutian Range of south-central Alaska: U.S. Geological Survey Data Release. https://doi.org/10.5066/P96762V3

Jones, J.V., III, and O'Sullivan, Paul, 2020, U-Pb isotopic data and ages of zircon, titanite, and detrital zircon from rocks from the Yukon-Tanana Upland, Alaska: U.S. Geological Survey Data Release. https://doi.org/10.5066/P9WWV93S

Jones, J.V., III, Todd, Erin, Caine, J.S., Holm-Denoma, C.S., Ryan, J.J., and Benowitz, J.A., 2017, Late Permian (ca. 267–257 Ma) magmatism, deformation, and metamorphism and lithotectonic associations of the Ladue River unit in east-central Alaska [abs.]: Geological Society of America Abstracts with Programs, v. 49, no. 6. https://doi.org/10.1130/abs/2017AM-304170

Meschede, Martin, 1986, A method of discrimination between different types of mid-ocean ridge basalts and continental tholeiites with the Nb-Zr-Y diagram: Chemical Geology, v. 56, p. 207–218.

Naibert, T.J., Benowitz, J.A., Wypych, Alicja, Sicard, K.R., and Twelker, Evan, 2018, $^{40}Ar/^{39}Ar$ data from the Tanacross D-1 and D-2, Big Delta B-4 and B-5, and Mount Hayes A-6 quadrangles, Alaska: Alaska Division of Geological & Geophysical Surveys Raw Data File 2018-3, 15 p. https://doi.org/10.14509/30112

Naibert, T.J., Benowitz, J.A., Wypych, Alicja, Sicard, K.R., and Twelker, Evan, 2020, $^{40}Ar/^{39}Ar$ data from the Tanacross D-1 and parts of the D-2, C-1, and C-2 quadrangles, Alaska: Alaska Division of Geological & Geophysical Surveys Raw Data File 2020-12, 35 p. https://doi.org/10.14509/30466

Naibert, T.J., Wypych, Alicja, Newberry, R.J., Twelker, Evan, Gavel, M.M., Wildland, A.D., Barrera, M.L., Szumigala, D.J., Regan, S.P., Avirett, D.F., Bernard, C.M., Blackwell, N.J., Fessenden, S.N., Harvey, D.A., Hubbard, A.K., Masterman, S.S., Muller, I.P., Turner, M.M., and Wyatt, W.C., 2024, Geologic background and map unit descriptions to accompany bedrock geologic maps of the western Tanacross and Taylor Mountain areas, Tanacross and Eagle quadrangles, Alaska, *in* Naibert, T.J., ed., Geologic investigation of the Western Tanacross and Taylor Mountain areas, Tanacross and Eagle quadrangles, Alaska: Alaska Division of Geological & Geophysical Surveys Preliminary Interpretive Report 2024-6A, 39 p. https://doi.org/10.14509/31167

Newberry, R.J., Bundtzen, T.K., Clautice, K.H., Combellick, R.A., Douglas, Tom, Laird, G.M., Liss, S.A., Pinney, D.S., Reifenstuhl, R.R., and Solie, D.N., 1996, Preliminary geologic map of the Fairbanks mining district, Alaska: Alaska Division of Geological & Geophysical Surveys Public Data File 96-16, 17 p., 2 sheets, scale 1:63,360. https://doi.org/10.14509/1740

Newberry, R.J., Bundtzen, T.K., Mortensen, J.K., and Weber, F.R., 1998, Petrology, geochemistry, age, and significance of two foliated intrusions in the Fairbanks District, Alaska, *in* Gray, J.E., and Riehle, J.R., eds., Geologic studies in Alaska by the U.S. Geological Survey, 1996: U.S. Geological Survey Professional Paper 1595, p. 117–129.

Newberry, R.J., and Twelker, Evan, 2021, Metamorphism of the Ladue River-Mount Fairplay area, *in* Twelker, Evan, ed., Geologic investigation of the Ladue River-Mount Fairplay area, eastern Alaska: Alaska Division of Geological & Geophysical Surveys Report of Investigation 2021-5B, p. 33–39. https://doi.org/10.14509/30736

Pavlis, T.L., Sisson, V.B., Foster, H.L., Nokleberg, W.J., and Plafker, George, 1993, Mid-Cretaceous extensional tectonics of the Yukon-Tanana Terrane, Trans-Alaska Crustal Transect (TACT), east-central Alaska: Tectonics, v. 12, p. 103–122.

Pearce, Julian, and Cann, Johnson, 1973, Tectonic setting of basic volcanic rocks determined using trace element analyses: Earth and Planetary Science Letters, v. 19, p. 290–300. https://doi.org/10.1016/0012-821X(73)90129-5

Piercey, S.J., Nelson, J.L., Colpron, Maurice, Dusel-Bacon, Cynthia, Simard, R.-L., and Roots, C.F., 2006, Paleozoic magmatism and crustal recycling along the ancient Pacific margin of North America, northern Cordillera, *in* Colpron, Maurice, and Nelson, JoAnne, eds., Paleozoic evolution and metallogeny of pericratonic terranes at the ancient pacific margin of North America: Geological Association of Canada, Special Paper 45, p. 281–322.

Smith, T.E., Robinson, M.S., Weber, F.R., Waythomas, C.F., and Reifenstuhl, R.R., 1994, Geologic map of the upper Chena River area, eastern interior Alaska: Alaska Division of Geological & Geophysical Surveys Professional Report 115, 19 p., 1 sheet, scale 1:63,360. https://doi.org/10.14509/2315

Solie, D.N., Werdon, M.B., Freeman, L.K., Newberry, R.J., Szumigala, D.J., Speeter, G.G., and Elliott, B.A., 2019, Bedrock-geologic map, Alaska Highway corridor, Tetlin Junction, Alaska to Canada border: Alaska Division of Geological & Geophysical Surveys Preliminary Interpretive Report 2019-3, 16 p., 2 sheets, scale 1:63,360. https://doi.org/10.14509/30038

Szumigala, D.J., Newberry, R.J., Werdon, M.B., Athey, J.E., Flynn, R.L., and Clautice, K.H., 2002, Bedrock geologic map of the Eagle A-1 Quadrangle, Fortymile mining district: Alaska Division of Geological & Geophysical Surveys Preliminary Interpretive Report 2002-1B, 1 sheet, scale 1:63,360. https://doi.org/10.14509/2864

Todd, Erin, Kylander-Clark, Andrew, Kreiner, D.C., Jones, J.V., III, Holm-Denoma, C.S., and Wypych, Alicja, 2023, U-Pb ages, hafnium isotope ratios, and trace element concentrations by Laser-ablation Split Stream (LASS) Analysis of igneous and metamorphic zircons from the Yukon-Tanana Upland, eastern Alaska: U.S. Geological Survey Data Release. https://doi.org/10.5066/P9O1DMIE

Todd, Erin, Wypych, Alicja, and Kylander-Clark, Andrew, 2019, U-Pb and Lu-Hf isotope, age, and trace element data from zircon separates from the Tanacross D-1, and parts of D-2, C-1, and C-2 quadrangles: Alaska Division of Geological & Geophysical Surveys Raw Data File 2019-5, 10 p. https://doi.org/10.14509/30198

Truskowski, C.M., Heizler, M.T., Naibert, T.J., Newberry, R.J., Twelker, Evan, and Szumigala, D.J., 2025, $^{40}Ar/^{39}Ar$ geochronology data from the Big Delta, Eagle, and Mount Hayes quadrangles, Alaska: Alaska Division of Geological & Geophysical Surveys Raw Data File 2025-11, 21 p. https://doi.org/10.14509/31534

Twelker, Evan, and O'Sullivan, P.B., 2021, U-Pb zircon data and ages for bedrock samples from the Richardson mining district, Big Delta Quadrangle, Alaska: Alaska Division of Geological & Geophysical Surveys Raw Data File 2020-14, 17 p. https://doi.org/10.14509/30555

Twelker, Evan, Newberry, R.J., Wypych, Alicja, Naibert, T.J., Wildland, A.D., Sicard, K.R., Regan, S.P., Athey, J.E., Wyatt, W.C., and Lopez, J.A., 2021a, Bedrock geologic map of the Ladue River-Mount Fairplay area, Tanacross and Nabesna quadrangles, Alaska, *in* Twelker, Evan, ed., Geologic investigation of the Ladue River-Mount Fairplay area, eastern Alaska: Alaska Division of Geological & Geophysical Surveys Report of Investigation 2021-5A, p. 1–32, 1 sheet, scale 1:100,000. https://doi.org/10.14509/30735

Twelker, Evan, Wildland, A.D., Werdon, M.B., Sicard, K.R., Wypych, Alicja, Naibert, T.J., Athey, J.E., Willingham, A.L., and Lockett, A.C., 2021b, Preliminary bedrock geologic map database, northeastern Richardson mining district, Alaska: Alaska Division of Geological & Geophysical Surveys Raw Data File 2021-9, 4 p. https://doi.org/10.14509/30676

Werdon, M.B., Newberry, R.J., and Szumigala, D.J., 2001, Bedrock geologic map of the Eagle A-2 Quadrangle, Fortymile mining district, Alaska: Alaska Division of Geological & Geophysical Surveys Preliminary Interpretive Report 2001-3B, 1 sheet, scale 1:63,360. https://doi.org/10.14509/2670

Werdon, M.B., Newberry, R.J., Athey, J.E., and Szumigala, D.J., 2004, Bedrock geologic map of the Salcha River-Pogo area, Big Delta Quadrangle, Alaska: Alaska Division of Geological & Geophysical Surveys Report of Investigation 2004-1B, 19 p., 1 sheet, scale 1:63,360. https://doi.org/10.14509/3209

Werdon, M.B., Solie, D.N., Newberry, R.J., Freeman, L.K., Elliott, B.A., and Lessard, R.R., 2019, Bedrock-geologic map, Alaska Highway corridor, Little Gerstle River to Dot Lake, Alaska: Alaska Division of Geological & Geophysical Surveys Preliminary Interpretive Report 2019-1, 12 p., 1 sheet, scale 1:63,360. https://doi.org/10.14509/30036

Wildland, A.D., 2022, Temporal links between ductile shearing, widespread plutonism, and tectonic exhumation near the boundary of parautochthonous and allochthonous terranes in the northern Cordillera, Alaska: Fairbanks, Alaska, University of Alaska Fairbanks, M.S. thesis, 67 p.

Wildland, A.D., Wypych, Alicja, Regan, S.P., and Holland, Mark, 2021, U-Pb zircon ages from bedrock samples collected in the Tanacross and Nabesna quadrangles, eastern Alaska: Alaska

Division of Geological & Geophysical Surveys Preliminary Interpretive Report 2021-4, 47 p. https://doi.org/10.14509/30732

Wilson, F.H., Hults, C.P., Mull, C.G., and Karl, S.M., 2015, Geologic map of Alaska: U.S. Geological Survey Scientific Investigations Map 3340, 196 p., 2 sheets, scale 1:1,584,000. https://alaska.usgs.gov/science/geology/state_map/interactive_map/AKgeologic_map.html.

Wypych, Alicja, Hubbard, T.D., Naibert, T.J., Athey, J.E., Newberry, R.J., Sicard, K.R., Twelker, Evan, Werdon, M.B., Willingham, A.L., Wyatt, W.C., and Lockett, A.C., 2021, Northeast Tanacross geologic map and map units and descriptions, *in* Wypych, Alicja, ed., Northeast Tanacross geologic mapping project, Alaska: Alaska Division of Geological & Geophysical Surveys Report of Investigation 2020-9B, p. 9–26, 1 sheet, scale 1:63,360. https://doi.org/10.14509/30539

Wypych, Alicja, Jones, J.V., III, and O'Sullivan, Paul, 2020, U-Pb zircon ages from bedrock samples collected in the Tanacross D-1, and parts of the D-2, C-1, and C-2 quadrangles, Alaska: Alaska Division of Geological & Geophysical Surveys Preliminary Interpretive Report 2020-2, 19 p. https://doi.org/10.14509/30465

Wypych, Alicja, Naibert, T.J., Athey, J.E., Newberry, R.J., Sicard, K.R., Twelker, Evan, Werdon, M.B., Willingham, A.L., and Wyatt, W.C., 2018, Major-oxide and trace-element geochemical data from rocks collected in 2018 for the Northeast Tanacross project, Tanacross C-1, C-2, D-1, and D-2 quadrangles, Alaska: Alaska Division of Geological & Geophysical Surveys Raw Data File 2018-4, 4 p. https://doi.org/10.14509/30113

Wypych, Alicja, Twelker, Evan, Naibert, T.J., Gavel, M.M., Newberry, R.J., Szumigala, D.J., Wildland, A.D., Barrera, M.L., Harvey, D.A., Muller, I.P., Fessenden, S.N., and Blackwell, N.J., 2023, Geochemical data from samples collected in 2022 for the Mount Harper geologic mapping project, Big Delta, Mount Hayes, and Eagle quadrangles, Alaska: Alaska Division of Geological & Geophysical Surveys Raw Data File 2023-24, 3 p. https://doi.org/10.14509/31089

Wypych, Alicja, Naibert, T.J., Newberry, R.J., Twelker, Evan, Gavel, M.M., Wildland, A.D., Szumigala, D.J., Regan, S.P., Avirett, D.F., Barrera, M.L., Bernard, C.M., Blackwell, N.J., Fessenden, S.N., Harvey, D.A., Hubbard, A.K., Masterman, S.S., Muller, I.P., Turner, M.M., and Wyatt, W.C., 2024, Bedrock geologic map of the Western Tanacross area, Tanacross Quadrangle, Alaska, *in* Naibert, T.J., ed., Geologic investigation of the Western Tanacross and Taylor Mountain areas, Tanacross and Eagle quadrangles, Alaska: Alaska Division of Geological & Geophysical Surveys Preliminary Interpretive Report 2024-6C, 1 sheet, scale 1:100,000. https://doi.org/10.14509/31169

Yukon Geological Survey, 2019, Yukon bedrock geology map: Yukon Geological Survey webmap, accessed March 19, 2019, https://yukon.ca/en/yukon-geology#bedrock-geology.